DESIGN OPTIMIZATION OF SPEED INCREASER INSTALLED ON WIND POWER GENERATOR

WANG LESU

THESIS SUBMITTED IN FULFILMENTOF THE REQUIREMENTS FOR THE DEGREE OF MASTER OF MACHANICAL ENGINEERING

FACULTY OF ENGINEERING

UNIVERSITY OF MALAYA

KUALA LUMPUR

2019

<div align="center">

UNIVERSITY OF MALAYA

ORIGINAL LITERARY WORK DECLARATION

</div>

Name of Candidate: **WANG LESU**

Matric No: **KQK170035**

Name of Degree: **Master of Mechanical Engineering**

Title of Project Project/Research Report/Dissertation/Thesis ("this Work"):

Design Optimization of Speed Increaser Installed on Wind Power Generator

Field of Study: **Finite Element Analysis**

I do solemnly and sincerely declare that:

  (1) I am the sole author/writer of this Work;

  (2) This Work is original;

  (3) Any use of any work in which copyright exists was done by way of fair dealing and for permitted purposes and any excerpt or extract from, or reference to or reproduction of any copyright work has been disclosed expressly and sufficiently and the title of the Work and its authorship have been acknowledged in this Work;

  (4) I do not have any actual knowledge nor ought reasonably to know that the making of this work constitutes an infringement of any copyright work;

  (5) I hereby assign all and every rights in the copyright to this Work to the University of Malaya ("UM"), who henceforth shall be owner of the copyright in this Work and that any reproduction or use in any form or by any means whatsoever is prohibited without the written consent of UM having been first had and obtained;

  (6) I am fully aware that if in the course of making this Work I have infringed any copyright whether intentionally or otherwise, I may be subject to legal action or any other action as may be determined by UM.

Candidate's Signature   Date:

Subscribed and solemnly declared before,

Witness's Signature   Date:

Name:

Designation:

Design Optimization of Speed Increaser Installed on Wind Power Generator

ABSTRACT

Wind power speed increaser is a low-speed and heavy-duty gear transmission equipment. It serves as one of the important components in wind turbine. The working environment and characteristics determine that it often breaks down after long term operation. Therefore, the design, reliability and dynamics of wind power speed increaser are highly demanded. Thus, the static analysis & dynamic analysis are used to check the safety of increaser and optimization are used to improve the reliability of it. This study used Shigley's design method and computational analysis (FEA) to analyze the feasibility of the design. Safety factor was calculated by Shigley's design method; static analysis, dynamic analysis and design optimization were carried out by using ANSYS Workbench 18.0 software. The speed increaser was analyzed on safety factors, maximum stress & maximum deformation of gears, shafts, keys and casing. Based on the Shigley's design methods, the results have shown that gears, shafts, keys and bearing do not have any failure. For computational analysis, all gears, bearing and casing also do not indicate any failure in static analysis and dynamic analysis. However, it is noted that the equivalent stress of shaft III is too large reaching 1148.5 MPa and the fatigue safety factors of shaft III and key III is 0.33 and 1.03, respectively, which indicates fatigue failure is likely happen in these machine components. The problems are mainly focused on the strength failure. Design optimization is focused on reducing stress and increasing safety factor. The diameter and fillet of shaft, length and width of key are used as input parameters. The best candidate from the design optimization analysis showed a positive result by increasing diameter of shaft and increasing length and width

of key. The fatigue safety factor of shaft increased to 1.4 and stress reduces to 279.64MPa. The fatigue safety factor of key also increased to 1.48.

**Pengoptimuman Reka Bentuk Peningkatan Kelajuan
Dipasang pada Penjana Kuasa Angin**

ABSTRAK

Sebagai salah satu komponen penting turbin angin, peningkatan kelajuan kuasa Wwind adalah sejenis peralatan transmisi gear berkelajuan rendah dan berat. Ia berfungsi sebagai salah satu komponen penting dalam turbin angin. Persekitaran kerja dan ciri-ciri menentukan bahawa ia sering terputus dalam proses penggunaan proses jangka panjang. Oleh itu, reka bentuk, kebolehpercayaan dan dinamik peningkatan tenaga kuasa angin sangat dituntut. Oleh itu, analisis statik, analisa dinamik dan pengoptimuman reka bentuk peningkatan kelajuan adalah kepentingan penting yang besar untuk memperbaiki meningkatkan kebolehpercayaan. Kajian ini menggunakan pengiraan manual dan analisis komputasi (FEA) untuk menganalisis kemungkinan reka bentuk. Faktor keselamatan dihitung dengan pengiraan manual; analisis statik, analisis dinamik dan pengoptimuman reka bentuk dijalankan dengan menggunakan perisian ANSYS Workbench 18.0. Untuk memudahkan analisis, makalah ini membahagi-bahagikan kelajuan membahagi dianalisis pada gear, tiang, kunci, galas dan selongsongnya. Berdasarkan pengiraan manual, penganalisis menganalisis bahawa gear, aci, kunci dan galas tidak mempunyai kegagalan pada pengiraan manual. Untuk analisis pengkomputeran, semua gear, galas dan selongsong tidak dinyatakan tidak menunjukkan kegagalan dalam analisis statik dan analisis dinamik. Walau bagaimanapun, diperhatikan bahawa tetapi tekanan setara aci III adalah terlalu besar yang mencapai 1148.5 MPa dan faktor keselamatan yang lemah dari aci III dan kekunci III adalah di bawah 1 yang menunjukkan kegagalan keletihan mungkin berlaku dalam komponen mesin ini. Masalahnya tertumpu pada kepekatan tekanan di kawasan tajam

dan kegagalan kekuatan. Pengoptimuman reka bentuk ditumpukan untuk mengurangkan tekanan dan meningkatkan faktor keselamatan. Diameter dan fillet aci, panjang dan lebar kekunci digunakan sebagai parameter input. Calon terbaik pengoptimuman dari analisis pengoptimuman reka bentuk menunjukkan hasil positif dengan meningkatkan diameter batang dan meningkatkan panjang dan lebar kunci. Faktor keselamatan lelah aci meningkat kepada 1.4 dan tekanan menurun kepada 279.64MPa. Faktor keselamatan yang lemah juga meningkat menjadi 1.48.

ACKNOWLEDGEMENTS

I would like to give my greatest appreciation to my supervisor, Ir. Dr. Ong Zhi Chao for his valuable suggestions during the planning and development of this research project. I really appreciate his devotion of time and great willingness to spare no effort to help me.

My sincere thanks also go to University of Malaya, Faculty of Engineering and Department of Mechanical Engineering for offering me the opportunities to study in Malaysia and all the resources on doing my research project. In addition, I thank my classmates in University of Malaya: Omar Almatar Abd, Wang Yi Ming, Sivanesh kumar, Chin Chong Ho, Gao Wei, Lim Chin Xian and Badruzzaman for their supporting and encouragement. Also, I am very grateful to my parents and relatives for their support and concern. They are my driving force and solid backing. I wish them good health and all the best. Last, I sincerely thank all the experts and professors for their comments and criticisms in this busy schedule.

Thank you.

CONTENTS

LIST OF FIGURES

LIST OF TABLES

LIST OF SYMBOLS AND ABBREVIATIONS

S_F	:	Bending safety factor
S_H	:	Pitting safety factor
W^t	:	Transmitted load
P_d	:	Diametric pitch
N_P	:	The number of tooth
H	:	Power
σ	:	Gear bending stress
K_0	:	Overload factor
K_v	:	Dynamic factor
K_s	:	Size factor
K_m	:	Load-distribution factor
K_B	:	Rim-thickness factor
J	:	Geometry factor
S_t	:	Allowable bending stress number
Y_N	:	Stress-cycle factor
K_T	:	Temperature factor
K_R	:	Reliability factor
σ_c	:	Gear contact endurance stress
C_p	:	The elastic coefficient
C_f	:	Surface condition factor
I	:	Geometry factor
F	:	Net face width of narrowest member
S_C	:	AGMA surface endurance stress
Z_N	:	Stress-cycle factor
C_H	:	Hardness-ratio factor
σ_a	:	The alternating stress
σ_m	:	The mean stress
K_f	:	Fatigue stress-concentration factor
M_a	:	Maximum moment

K_{fs}	:	Fatigue stress-concentration factor
T_a	:	Torque
M_m	:	Moment
T_m	:	Maximum torque
S_e	:	The endurance limit
S'_e	:	Rotary-beam test specimen endurance limit
k_a	:	Surface condition modification factor
k_b	:	Size modification factor
k_c	:	Load modification factor
k_d	:	Temperature modification factor
k_e	:	Reliability factor
k_f	:	Miscellaneous-effects modification factor
n_f	:	Factor of safety of fatigue failure
S_{ut}	:	The yield strength
n_y	:	Factor of safety of yielding
S_y	:	Yield limit strength
S_{sy}	:	Shear strength
σ_y	:	The yield stress
$\overline{\sigma}$	:	The von Mises stress
t	:	Thickness
l	:	Length
C_{10}	:	Rated dynamic load
a_f	:	Application factor
F_D	:	Design load
$X(t)$	:	Displacement
$\dot{X}(t)$	:	Velocity
$\ddot{X}(t)$	:	Acceleration
σ_1	:	The maximum principal stress

σ_2	:	The minimum principal stress
UGNX	:	Name of a 3D modeling software
42CrMo	:	Ultra high strength steel
QT400	:	Ductile iron
kg	:	Kilogram
mm	:	Millimeter
kW	:	Kilowatt
rev/min	:	Rev per minute
$\dfrac{N_F}{N_E}$	:	Tooth number ratio
N.m	:	Moment
C_0	:	Basic rated static load
P_u	:	Fatigue load limit
ω	:	Speed of shaft, rev/min
Hz	:	Frequency
q	:	Notch sensitivity
q_s	:	Notch sensitivity of shear

CHAPTER 1: INTRODUCTION

1.1   The Research Background

Speed increaser is a kind of speed-up gearbox. In wind power generator, speed increaser is the core transmission component. its main function is to connect the wind turbine and the generator. By reducing the torsion and increasing the speed of the gearbox, the speed and torque matching the generator are output, and the power generated by wind energy is transmitted to the generator, which is ultimately transformed into electric energy.

In various parts of the wind turbine, the speed increaser component has the highest failure rate, and it is also the main bottleneck in the design of wind power generation in the world. At present, the failure of speed increaser mainly concentrated on that the working life is less than the design requirements. The design life of many speed increasers are 60 years. But because the breakage and corrosion of gears and shafts, the working life is always less than design life. The failures of gears and shafts are the major reasons to cause speed increaser fault. Therefore, it is important to use effective method to check the problems on the gears, shaft &keys of the speed increaser. And if it has problems, the optimization is used to change the structure of components of speed increaser to solve the problems (Liu, Z., 2010).

With the global energy consumption increasing year by year, environmental pollution is becoming more and more serious, and countries around the world pay more

attention to the use of wind energy. According to the latest wind power installed data released by the Global Wind Energy Council (GWEC), the installed capacity in 2016 exceeded 54.6 million kilowatts. From the cumulative installed capacity point of view, the increase in just 16 years is as high as 20 times, which shows the importance of the use of wind turbines (Wei, W. , 2017).

Wind power is becoming an important part of power generation because of the limitation of fossil fuels and the pollution. Also there are many advantages on wind power generator (Figure1.1) such as low cost of generating electricity and suitable for large scale installation, which is good for improving energy structure. The gear speed increaser is the main driving part in wind turbine; therefore, the design of the speed increaser is an important factor in the efficient work of the wind turbine (Bao, E., 2004).
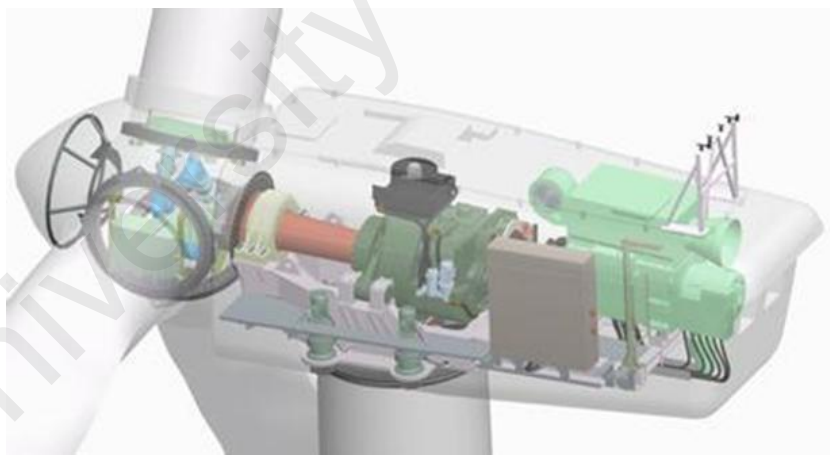
Figure1.1: Overview of wind power generator.

In 1880, the first planetary gear train appeared in Germany. With the development of the machinery industry, especially the automobile and aircraft industry, the development of the planetary gear train has also changed a lot. In 20th, high speed and low speed heavy load planetary transmission device had been produced in Germany and

Japan. 300 kW wind turbines are mainly used in coastal areas where transportation and installation conditions are not ideal. 600 kW wind turbines are mainly used in areas with flat terrain. 1500 kW wind generator has good economic benefits. According to the installation form of wind turbine shaft, the current wind power generation equipment is mainly divided into two types: Horizontal Axis Wind Turbine and Vertical Axis Wind Turbine (Zhao, X., Liang, Y. W. & Lee, S. S., 2009).

The speed increaser analyzed in this project is installed on the WT1500-D28 wind turbines manufactured by China Power Grid Corporation. The wind power generation is Horizontal Axis Wind Turbine. The structure, components and main parameters of the speed increaser will be introduced in chapter2 literature review.

1.2   Problem Statement

Wind power generation gear box is a kind of low-speed, heavy load and speed increasing gear transmission device operated by irregular wind direction. Wind turbines are usually installed in the wilderness, the wild, the mountain pass and the seaside (Wang, J. J., & Wu, X. L., 2008). And the gearbox was installed in the narrow cabin of the tower, which is tens of meters above the ground and even one hundred meters high. Gear box is affected by bad natural environment and hard to repair. If the gearbox fails during the peak period of power generation, which will seriously affect the economic benefits of wind power generation. According to the statistics of actual operation of wind turbines in recent years, the failure rate of gearbox in wind turbines is as high as

9.8% (Crabtree, C. J., Feng, Y., & Tavner, P. J., 2010). And because the gear box repair program is the most complex, its failure caused by the downtime accounted for 19.4% of the total downtime (Figure 1.2). Also, the failures of wind power gearbox are often manifested as gear tooth breakage, pitting corrosion, input shaft breakage, high-speed shaft leakage, bearing burns (Lee,Y., Zhu,C.Z., & Tao,Y.C., 2017). Therefore, customers ask high requirements for reliability and service life of gearboxes and gear boxes need to be further studied.

b). Failure rate statistics of core components

Gear box 9.8%
Yaw system 6.7%
Electronic system 17.5%
Sensor 14.1 %
Blade 13.4%
Hydraulic pressure 13.3%
Control system 12.9%
Others 12.3%

a). Core component downtime statistics

Gear box 19.4%
Yaw system 13.3%
Electronic system 14.3%
Sensor 5.4%
Blade 9.4%
Hydraulic pressure 8.9%
Control system 18.3%
Others 11%
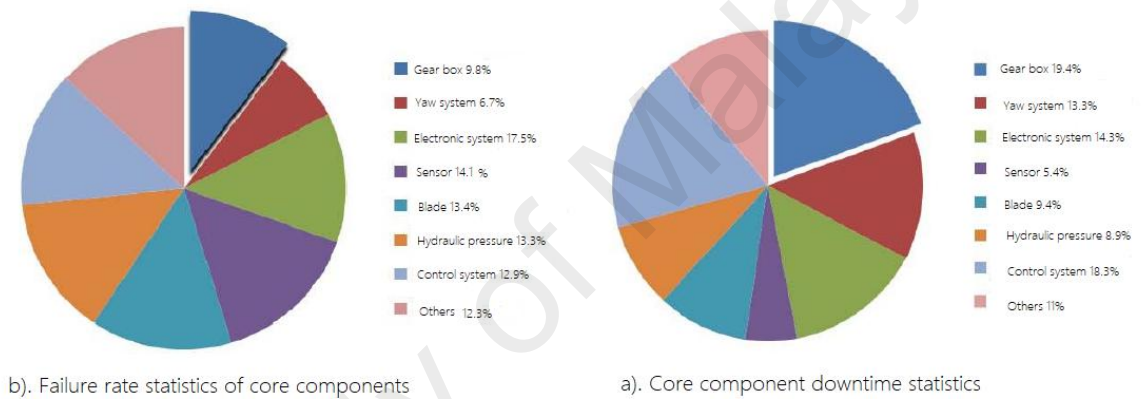
Figure1.2: Faults and downtime of core components of wind turbine.

With the development of technology, the requirements for the strength, vibration and noise of the speed increaser are stricter. Many studies have shown that the vibration and noise of the gear drive are mainly caused by the vibration of the gear box driven by the dynamic load. The vibration level of the gear system is directly related to the noise emitted by the gear device (Mabie, H. H., & Reinholtz, C. F., 1987).

The finite element analysis of the shafting system provides a powerful tool for the evaluation of its dynamic characteristics and performance, which can be used as an effective standard for product performance evaluation (Wu, J. L., 2005). According to the results of the finite element analysis, the parameters can be identified. Its task is to

4

determine the parameters of the vibration system from the data obtained from the test, including model natural frequency, modal damping ratio and mode shape. The static analysis can help to analyze the static safety factor and maximum stress of components of speed increaser; dynamic analysis can help to analyze the nature frequency and harmonic response of it; parameter optimization by using ANSYS software can help to solve the problems (low safety factor & high stress) by changing dimensions (Lin, J., & Parker, R. G., 2002).

The working life is less than the design requirements; the failures are often found as gear tooth breakage, pitting corrosion, shaft breakage, and bearing burns; the vibration and noise of the gear are mainly caused by the dynamic load are the main problems. Mechanical design and optimization can help to solve these problems (Figure 1.3).
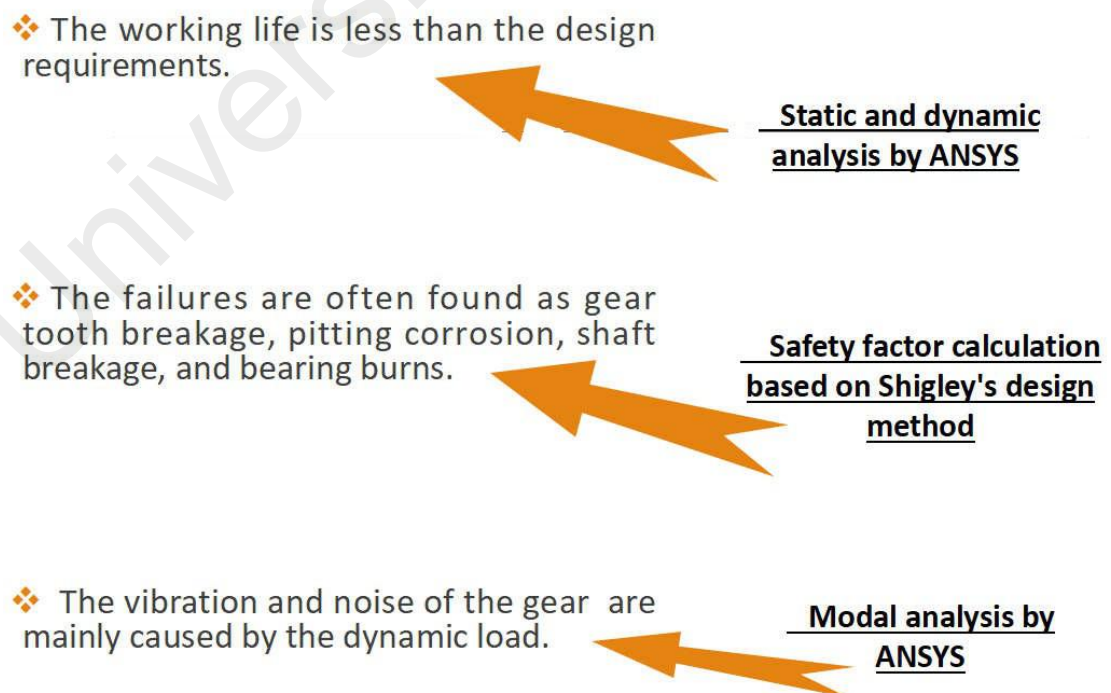
Figure1.3: How to solve problems.

1.3   Research Objectives

The objectives of this study:

   a). To design and build model of the speed increaser in wind power generation.

   b). To analyze the stress and safety factor of the speed increaser based on Shigley's Design Method.

   c). To perform static analysis and dynamic analysis on speed increaser: evaluate the static performance and dynamic performance in terms of vibration and fatigue failure.

   d). To enhance the design of the speed increaser: the maximum equivalent stress, safety factor, the vibration of the machine and the working life of this speed increaser can be optimized.

1.4   Research Scope

   The scope of this study is due to analyzing the speed increaser by using Shigley's design method and computational analysis methods. It is also needed to build the speed increaser model by using UGNX 10.0 software. Then, ANSYS software will be used to perform optimization. The analysis of this project is divided into 2 methods: (i) Shigley's design method of gears, shafts, keys and bearing; (ii) Computational analysis of gears, shafts, keys, bearings and casing. Because, Shigley's design method is a best way to calculate the stress and safety factor of mechanical components by substituting the related parameters. FEA method analyzes the static and dynamic characteristics of the parts in detail, which can show the specific location of the maximum stress and breakage place. These two methods are very helpful in finding problems in speed increaser. The model of the components will be analyzed by using ANSYS Workbench

18.0 software. Shigley's design method will be used to carry out the factor of safety of components. Static analysis will be used to analyze the stress and safety factor from stress tool. Fatigue failure analysis will be carried out to analyze safety factor from fatigue tool. And the natural frequency of the geometry will be obtained from Modal analysis. Optimization is used to solve the problem of low safety factor.

After analyzing and optimizing the speed increaser in this project, some components can be initially checked for damage or failure. The parts with insufficient safety factor and large stress can be found. Optimization by ANSYS software can help parts solve failure problems and improve safety factor. Through analysis and optimization, the safety and durability of speed increaser are improved. At the same time, its working life is checked to achieve the design working time.

1.5   Thesis Outline

This project consists of five chapters. The layout of the article shows the research process and the overall structure. Chapter 1 describes the background information of the research and the problems that the research is facing at present, and explains the reasons for the problems and remains to be solved. This research is devoted to solving the problem and optimizing the accelerator.

In addition, the content of Chapter 2 is mainly devoted to reviewing other research literature in this field, which is conducive to understanding the research level in this field. Literature review is mainly to help understand the research field, which comes

from journals, projects and books. This chapter compares the optimization methods from other studies. Besides, the Shigley's design method theory, static analysis theory, fatigue failure theory and modal analysis theory are introduced.

In chapter 3, the design of the accelerator and the parameters of each part are discussed in detail, and the working principle of the accelerator is explained. The Shigley's design method method is emphasized. The model of speed increaser will be built using UGNX software. ANSYS workbench 18 will be used for static analysis, fatigue failure analysis, modal analysis, and parameter optimization.

In chapter 4, the results will be analyzed and discussed from two aspects of Shigley's design method and computational analysis. The optimization results are also presented.

Chapter 5 summarizes the research of the whole project, and summarizes the research results and future work of the subject.

CHAPTER 2: LITERATURE REVIEW

In this chapter, the main purpose is solving the problems below:

1. Structure & parameter of speed increaser;

2. Analysis methods of speed increaser;

   a. Analysis components based on Shigley's design method.

   b. Analysis components for static and dynamic analysis with FEA method based on computational analysis.

3. Design optimization and structure optimization in ANSYS software.

2.1   Structure & Parameter of Speed Increaser

The speed increaser analyzed in this project is installed on the WT1500-D28 wind turbine manufactured by China Power Grid Corporation. The wind power generation is Horizontal Axis Wind Turbine. All parameters of the speed increaser are from design drawing of WT1500-D28 wind turbine.

She, B. Q. (2008) described that there are many kinds of speed increaser for wind turbines. According to the traditional types, they can be divided into cylindrical gearboxes, planetary gearboxes and their combined gearboxes. According to the series of transmission, they can be divided into single-stage and multi-stage gearboxes. According to the distribution form of transmission, it can be divided into expansion type, shunt type and coaxial type. Commonly used gear distribution forms are shown in Table 2.1.

Table 2.1: Commonly used gear distribution forms.(She, B. Q. , 2008)

	Sketch	Characteristic
Expansion type		The structure is simple, but the position of the gear relative to the bearing is not symmetrical. Therefore, the shaft is required to have a great stiffness.
Shunt type		The structure is complex, but because the gears are symmetrically distributed relative to the bearings, the bearings are loaded uniformly.
Coaxial type		The transverse dimension is small, the axial dimension and weight are large, and the load distribution on the teeth is not uniform.

At present, the 10kW's gearbox adopts 2K-H (NGW) planetary gear transmission whose input shaft is planet carrier and output shaft is solar wheel. And the speed increaser above 500kW usually use power split planetary transmission. 500kW-1000kW's common structures are "two stage parallel shelf + a planetary gear" and "one stage parallel shelf + two stage planetary gears". The speed increaser box of 1500kW wind turbine adopts "Two level parallel shelf + a planetary gear" structure (Zhan, Z., 2003).

The speed increaser studied in this project is a multi-stage gearbox with "Two level parallel shelf + a planetary gear" structure . For cylindrical gears, the gear distribution form is selected as expansion type. The sketch of transmission structure of speed increaser is shown below on Figure 2.1.
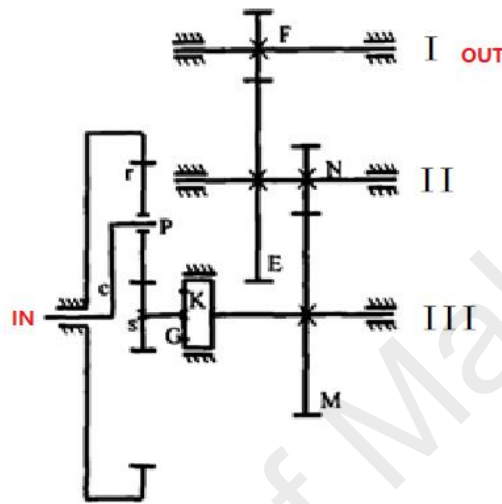
Figure 2.1: Sketch of transmission structure of speed increaser

She, B. Q. (2008) described that load and strength of material are two important factors determining the factor of safety. In this speed increaser, there are two main material used in components, which are Ultra-high Strength Steel (42CrMo) and Ductile iron (QT400). Ultra-high Strength Steel is used in gears, shafts and keys. Ductile iron is used in casing. The parameters of the materials are introduced below on the Table 2.2.

Table 2.2: Parameters of materials (She, B. Q. , 2008).

Material	Density kg/m^3	Young's modulus (Pa)	Poisson's ratio	Tensile yield strength (Pa)	Tensile ultimate yield strength (Pa)	Hardness (Brinell)
Ultra-high Strength Steel (42CrMo)	7850	2.12E+11	0.280	9.3E+08	1.08E+09	320
Ductile iron (QT400)	7200	1.61E+11	0.274	2.5E+08	4.0E+08	-

The speed increaser analyzed in this project is installed on the WT1500-D28 wind turbines manufactured by China Power Grid Corporation, therefore, the parameters of each components in speed increaser are known. From the WT1500-D28 wind turbines' product specifications and design drawings, the parameter of gears, shafts and keys are shown below:

Rated power: 1500kW; Input speed: 20 rev/min; Output speed: 1500 rev/min; Wind turbine design speed: 20 rev/min; Rated speed of generator: 1500 rev/min.

Important parameters of gears: (Guo, X. W. , 2012)

The out power of this wind power generation is 1500Kw.

The thickness of all gears is 300 mm.

The number of gear teeth   F   is 20, modulus= 8 mm

The number of gear teeth   E   is 90, modulus= 8 mm

The number of gear teeth   N   is 22, modulus= 10 mm

The number of gear teeth   M   is 94, modulus= 10 mm

The number of gear teeth   S   is 23, modulus= 16 mm

The number of gear teeth   P   is 34, modulus= 16 mm

Because of the formula: $T = \dfrac{9549 \times P}{n}$ N · m

Where,   T is torque,   Nm

n is speed of gear,   r/min

P is translate power,   kW

The input speed is 20 r/min.

The output speed is 1500 r/min.

The mechanical efficiency is 95%

So, the moment on Gear E is: $T_E = \frac{9549 \times 1500}{1500 \times 95\%} \times \frac{90}{20} = 45230 \text{ N} \cdot \text{m}$

the moment on Gear M is: $T_M = \frac{45230}{95\%} \times \frac{94}{22} = 203425 \text{ N} \cdot \text{m}$

the moment on input shaft is: $T_{in} = \frac{202425}{95\%} \times \frac{91}{23} = 847215 \text{ N} \cdot \text{m}$

The diameters on mounting bearing position of shaft I, shaft II and shaft III are 120mm.

She, B. Q. (2008) analyzed the heat treatment characteristics of gears. Gear blank is made by forging method, which can obtain good forging structure fiber and corresponding mechanical properties. Reasonable heat treatment method is adopted to ensure that the comprehensive mechanical properties of the material can meet the design requirements. These two parameters of allowable bending stress number S_t & allowable contact stress number S_c are defined of the material used in gears. Table 2.3 lists the material properties of the gears in this project.

Table 2.3: The material properties of the gears (She, B. Q. , 2008).

	Material	Heat treatment	allowable bending stress number S_t	allowable contact stress number S_c
Gears	Ultra-high Strength Steel (42CrMo)	Tempering HB320-350 Tooth surface hardening HRC58-62	900 MPa	1650 MPa

2.2   Theories of Shigley's design method

Shigley's design method theories of speed increaser will be introduced in this part. They are Shigley's design method of gears based on AGMA standard, Shigley's design method of shafts, Shigley's design method of keys and Shigley's design method of bearing.

Continue the case study by specifying appropriate gears and shafts, this project specifies that components with safety factor greater than 1.2 are qualified (safety factor > 1.2). Achieve safety factors of at least 1.2 for pitting and bending safety factors of gears, shown below on Table 2.4. Achieve safety factors of at least 1.2 for yield and fatigue safety factor of shafts & keys (Richard, G. B., & Nisbett, J. K., 2010).

Table 2.4: The minimum pitting and bending safety factor.

Minimum safety factor for pitting fatigue of gears S_H	Minimum safety factor for bending fatigue of gears S_F
1.2	1.2

2.2.1   Calculation of Gears Based on AGMA Standard

Description of the procedure based on the AGMA standard is highly detailed. The best review is a "road map" for bending fatigue and contact-stress fatigue. These will be shown next: the bending stress equation, the endurance strength in bending equation, and the factor of safety S_F. Also, the contact-stress equation, the contact fatigue

endurance strength equation, and the factor of safety S_H will be displayed. When analyzing a gear problem, these equations are useful reference.

2.2.1.1 Spur gear bending analysis:

Based on ANSI/AGMA 2001-D04 (Richard, G. B., & Nisbett, J. K., 2010)

$$d_P = \frac{N_P}{P_d} \qquad \text{(Equation 2.1)}$$

$$V = \frac{\pi dn}{12} \qquad \text{(Equation 2.2)}$$

$$W^t = \frac{33000H}{V} \qquad \text{(Equation 2.3)}$$

Where,

d_p is diameter of gear,

N_p is the number of tooth,

P_d is diametric pitch,

V is rotating speed,

d is diameter,

n is rotating speed, rev/min,

W^t is force on gear tooth,

H is power.

Gear bending stress equation,

$$\sigma = W^t K_0 K_v K_s \frac{P_d}{F} \frac{K_m K_B}{J} \qquad \text{(Equation 2.4)}$$

Where,

K_0 is shown on Table 2.5,

K_v is dynamic factor, $K_v = (\frac{A+\sqrt{V}}{A})^B \qquad$ (Equation 2.5)

15

Table 2.5 Overload factor, K_0 (J. Keith Nisbett 2013)

Driven Machine			
Power source	Uniform	Moderate shock	Heavy shock
Uniform	1.00	1.25	1.75
Light shock	1.25	1.50	2.00
Medium shock	1.50	1.75	2.25

$$A = 50 + 56(1 - B)$$

$$B = 0.25(12 - Q_v)^{2/3}$$

Q_v is Gear Processing Accuracy,

K_s is size factor, $\quad K_S = 1.192(\frac{F\sqrt{Y}}{P})^{0.0535}$ (Equation 2.6)

K_m is Load-distribution factor,

F is net face width of narrowest member,

J is geometry factor,

$$K_m = 1 + C_{mc}(C_{pf}C_{pm} + C_{ma}C_e) ,$$ (Equation 2.7)

K_B is rim-thickness factor , $K_B = 1$, (Equation 2.8)

Gear bending endurance strength equation,

$$\sigma_{all} = \frac{S_t}{S_F} \frac{Y_N}{K_T K_R}$$ (Equation 2.9)

Where,

S_t is allowable bending stress number,

S_F is bending safety factor,

Y_N is stress-cycle factor,

K_T is temperature factor,

K_R is reliability factor.

Gear bending factor of safety,

$$S_F = \frac{S_t Y_N / (K_T K_R)}{\sigma}$$
(Equation 2.10)

2.2.1.2 Spur gear wear analysis

Based on ANSI/AGMA 2001-D04

Gear contact stress equation,

$$\sigma_c = C_p (W^t K_0 K_v K_s \frac{K_m}{d_p F} \frac{C_f}{I})^{1/2}$$
(Equation 2.11)

Where,

C_P is elastic coefficient, $C_P = \left[\dfrac{1}{\pi(\frac{1-v_p^2}{E_P} + \frac{1-v_G^2}{E_G})} \right]^{1/2}$
(Equation 2.12)

I is geometry factor, $I = \dfrac{cos\varphi \, sin\varphi}{2m_N} \dfrac{m_G}{m_G+1}$.
(Equation 2.13)

Gear contact endurance strength,

$$\sigma_{c,all} = \frac{S_C Z_N C_H}{S_H K_T K_R}$$
(Equation 2.14)

Where,

S_C is AGMAsurface endurance stress,

Z_N is stress-cycle factor,

C_H is hardness-ratio factor,

S_H is pitting safety factor,

K_T is temperature factor,

K_R is reliability factor.

Wear factor of safety,

$$S_H = \frac{S_C Z_N C_H / (K_T K_R)}{\sigma_c}$$

(Equation 2.15)

2.2.2 Shigley's design method of Shafts

Bending, torsion, and axial stress may be present in both mid-ranges and alternating components. For analysis, it is simple enough to combine the different types of stresses into alternating and mid-ranges von Mises stresses.

Combining the stress with the distortion energy failure theory, the von Mises stresses for rotating round, solid shafts, neglecting axial loads, are given by

The alternating stress: $\sigma_a = \left[(\frac{32 K_f M_a}{\pi d^3})^2 + 3(\frac{16 K_{fs} T_a}{\pi d^3})^2 \right]^{1/2}$ (Equation 2.16)

The mean stress: $\sigma_m = \left[(\frac{32 K_f M_m}{\pi d^3})^2 + 3(\frac{16 K_{fs} T_m}{\pi d^3})^2 \right]^{1/2}$ (Equation 2.17)

The endurance limit: $S_e = k_a k_b k_c k_d k_e k_f S_e'$ (Equation 2.18)

Where,

$$k_a = a S_{ut}^b$$

(Equation 2.19)

$$k_b = 1.51 d^{-0.157}$$

(Equation 2.20)

DE-Goodman failure criterion,

$$\frac{1}{n_f} = \frac{\sigma_a}{S_e} + \frac{\sigma_m}{S_{ut}}$$

(Equation 2.21)

Where,

n_f is factor of safety of fatigue failure

S_{ut} is the yield strength

18

Factor of safety of yielding,

$$n_y = \frac{S_y}{\sigma_a + \sigma_m}$$ (Equation 2.22)

2.2.3 Shigley's design method of Keys

Keys are used on shafts to secure rotating elements, gears and the keys are square keys. For safety the factor of safety is required above 1.5. Failure by shear across the area will create a stress of $\tau = \frac{F}{tl}$. Substitute the strength divided by the factor of safety for τ gets: (Richard, G. B., & Nisbett, J. K., 2010)

$$\frac{S_{sy}}{n} = \frac{F}{tl}$$ (Equation 2.23)

Where,

S_{sy} is shear strength.

n is factor of safety.

t is thickness, l is length.

To resist crushing, the area of one-half the face of the key is used:

$$\frac{S_y}{n} = \frac{F}{tl/2}$$ (Equation 2.24)

Where,

S_y is yield limit strength.

2.2.4 Shigley's design method of bearing

When the speed of shafts and the forces loaded on shafts are known, it is easy to select a suitable bearing by using Equation 2.25, which is from Shigley's bearing design method.

$$C_{10} = a_f F_D \left[\frac{x_D}{x_0 + (\theta - x_0)(1 - R_D)^{1/b}} \right]^{1/a}$$ (Equation 2.25)

Where,

a_f is application factor;

F_D is design load.

2.3   Theory of Computational Analysis

Some computational analysis theories will be introduced in this part. They are modal analysis theory, static failure theory and Goodman failure theory.

2.3.1   Modal Analysis

Modal analysis can be used to analyze the nature frequency of components. Every non-forced mechanical systems and stable systems with harmonic vibration at discrete frequencies are called natural frequencies. The analysis of vibration, modal analysis and frequency analysis are shown below:

Frequencies and mode shapes for undammed systems:

$$\begin{bmatrix} M_{11} & \cdots & M_{1n} \\ \vdots & \ddots & \vdots \\ M_{n1} & \cdots & M_{nn} \end{bmatrix} \begin{bmatrix} \ddot{X}_1 \\ \dots \\ \ddot{X}_n \end{bmatrix} + \begin{bmatrix} S_{11} & \cdots & S_{1n} \\ \vdots & \ddots & \vdots \\ S_{n1} & \cdots & S_{nn} \end{bmatrix} \begin{bmatrix} X_1 \\ \dots \\ X_n \end{bmatrix} = \begin{bmatrix} 0 \\ \dots \\ 0 \end{bmatrix} \qquad \text{(Equation 2.26)}$$

Assuming motion to be sinusoidal,

$$x_r = X_{Mr}\sin\left(\omega_{or}t + \varphi_1\right) \qquad \text{(Equation 2.27)}$$

Where,

$$x_r = \begin{bmatrix} X_1 \\ \dots \\ X_n \end{bmatrix}_r , \quad x_{Mr} = \begin{bmatrix} X_{m1} \\ \dots \\ X_{mn} \end{bmatrix}_r \qquad \text{(Equation 2.28)}$$

A multi degree of freedom system:

$$\text{M}\ddot{X} + C\ddot{X} + KX = f(t) \qquad \text{(Equation 2.29)}$$

$$\text{M}\ddot{u} + Ku = 0 \qquad \text{(Equation 2.30)}$$

Where,

M is the mass matrix;

C is the damping matrix;

K is the stiffness matrix;

f is the forcing vector;

u is the nodal displacement.

Assuming that the displacement varies with time,

$$\text{X(t)} = \overline{X}\sin{(\omega t)} \qquad \text{(Equation 2.31)}$$

$$\dot{X}(t) = \omega \overline{X}\cos{(\omega t)} \qquad \text{(Equation 2.32)}$$

$$\ddot{X}(t) = -\omega^2 \overline{X}\sin{(\omega t)} \qquad \text{(Equation 2.33)}$$

Where,

$\text{X(t)}, \dot{X}(t) \; and \; \ddot{X}(t)$ are displacement, velocity and acceleration.

Multiplying by using Equation 2.30 and the eigenvalue problem as shown in Equation 2.34 is generated.

$$[K - \omega_i{}^2 M]\overline{X_m} = 0 \qquad \text{(Equation 2.34)}$$

2.3.2 Von Mises Stress

The theory is called as maximum distortion energy theory. Von Mises stress has described as a single, equivalent, or effective stress for the entire general state of stress

21

in a stress element. Yielding happens when metal deformation occurs and the von Mises stress formulae is shown on Equation 2.35.

$$\bar{\sigma} = \frac{1}{\sqrt{2}}[(\sigma_1 - \sigma_2)^2 + (\sigma_2 - \sigma_3)^2 + (\sigma_3 - \sigma_1)^2]^{1/2}$$ (Equation 2.35)

Where,

σ_1 is the maximum principal stress,

σ_2 is the minimum principal stress.

And,

$$\bar{\sigma} \leq \sigma_y$$

2.3.3 Static Failure Theory

The factor of safety form stress tool can be determined from Equation 2.36 (Richard, G. B., & Nisbett, J. K., 2010).

$$n = \frac{\sigma_y}{\bar{\sigma}}$$ (Equation 2.36)

Where,

σ_y is the yield stress,

$\bar{\sigma}$ is the von Mises stress.

2.3.4 Goodman Failure Theory

Fatigue failure will be found when the stress focus on component is larger than the stress of the yield strength of materials. When the reciprocal of safety factor form fatigue tool is greater than the calculated parameters, the material can work safely. As shown below on Equation 2.37.

$$\frac{\sigma_a}{S_e} + \frac{\sigma_m}{S_{ut}} < \frac{1}{n} \qquad \text{(Equation 2.37)}$$

Where,

σ_a is the alternating stress,

σ_m is the mean stress,

S_e is the endurance limit,

S_{ut} is the yield strength and n is the factor of safety.

2.4 Common failure modes

Parey's study of the dynamics of Gear Transmission Systems focuses on defective gears such as pitting, palling and tooth breakage (2003). He established a dynamic model for the gears with the above-mentioned faults and analyzed the dynamic characteristics caused by various faults. But the dynamic model of this kind of fault gear is very difficult to establish, even if it is established, it is difficult to use the conventional analytical method to solve, only rely on some finite element software. The problem is that it is difficult to analyze the different response of gear systems above various conditions.

Ma, C., Ma, Y. L. & Zhao, H. A. (2011) introduced several common failure modes of gears in speed increaser.

1. Tooth surface wear;

Tooth surface wear is mainly caused by dust or metal particles or insufficient lubricant in the speed increaser, resulting in severe abrasive wear between the tooth surfaces. It makes the tooth profile of the gear change obviously, and causes the

meshing clearance to become bigger, and even causes the gear teeth to break because of the thinning of the gear teeth.

2. fatigue failure;

In the actual gear meshing process, relative rolling is accompanied by relative sliding, and the manifestations of fatigue failure are corrosion and flake corrosion. In the process of gear meshing, the contact stress of the tooth surface will change periodically. When the periodically varying contact stress exceeds the contact fatigue limit of the material, the contact surface of the gear will crack.

3. Tooth fracture;

The gear teeth bearing loads in the gearbox fail due to excessive impact, excessive load, or repeated bending stress. The failure form of spur gear is full teeth broken, while helical gear is partial broken.

Bao, E. (2004) mentioned in his article that because of the randomness and seasonality of wind speed, it will bring great uncertainty to the external excitation of the speed increaser. This kind of excitation makes the speed increaser produce great vibration and noise, which is also one of the most important reasons for the failure of the speed increaser.

2.5 Design Optimization

Design optimization is a process of structural optimization and parameter optimization for parts with failure or potential safety problems by using relevant technical methods. Before this study, many scholars devoted themselves to the

optimization design of the speed increaser, which solved many problems. But there are still many problems in the work of the speed increaser, such as breakage of gears & shafts, corrosion of gears and low working life. Through consulting the literature, it is known that the method combining Shigley's design method and computational analysis method has not been applied to analyze the components of the speed increaser. And optimization in ANSYS software will be a reasonable method to enhance safety factor.

Rossow, W. P., & Taylor, J. E. (2007) first used mathematical programming theory and finite element method to solve the minimum weight problem of elastic structures above multiple loads. Taylor have carried out the optimum design of the variable thickness stress film, and proposed the variable thickness method. However, this method is only suitable for optimizing objects such as plates and shells, and it is difficult to optimize three-dimensional continuum.

Sui, Y. K. (1996) proposed an independent continuous mapping method for the mutual transformation of discrete variables and continuous variables, using the idea of continuous topological variable change. And he established the topology optimization model of truss structure and solved the optimization design problem of truss structure above variable load and constraints.

Adam, M. R., & Magdi, R. (2010) took the planetary gear train and the box of the wind power gearbox as a system to optimize, and studied the influence of the system stiffness and the amount of gear misalignment on the optimization of the box.

Fuglsang, P. (2000) used constrained optimization method to optimize the structure of the box, established a mathematical model according to its working conditions, and achieved the goal of lightweight through iterative calculation.

Luo, H. T., Wang, C. J., Meng, J. H., & Zong, X. (2006) put forward the design method of institutional digitalization. From the point of view of system, he analyzed the mechanical components, improved the traditional design mode of isolation between analysis and design, provided a general design and development platform, realized the integration design and analysis of mechanical system, accelerated the design speed of products, and shortened the production cycle of mechanical products.

2.5.1　Structure Optimization

Mao, F. H., Han, M. K., & Dong, H. M. (2015) carried out lightweight research on the front body and the planetary frame of power split wind power gearbox, based on multi-position working conditions. He used topology optimization and size optimization methods to obtain lighter, better static characteristics of the new structure.

Guo, X. W. (2012) used 'Opti Struct' software, based on support vector machine theory and fruit fly optimization algorithm to carry out lightweight research on the traditional configuration of MW wind power gearbox. On the premise of guaranteeing the static and mechanical properties of the initial structure, he optimized the topology

and dimensions of the box and planetary frame, and finally got a new structural scheme of 3.67% weight reduction, which achieves the goal of lightweight.

Dong, H. M., Ding, S., & Wang, H. Y. (2014) studied the structural optimization of the central pillar, saddle and cross slide of CNC machine tools. Above the premise of ensuring the static and dynamic performance unchanged, they have achieved the goal of lightweight research of machine tools. Also, in the field of automotive structural optimization, they have established optimization models of suspension swing arm, body and transmission box, and carried out topology optimization and size optimization research.

Qin, D. T, Xing, Z. K., & Wang, J. H. (2008) considered the meshing stiffness, error and other factors, and established the optimization model of gearbox with the minimum volume as the objective function and the equal strength of gears as the constraint condition. He used MATLAB to analyze, above the condition of variable load, to achieve the purpose of greatly improving reliability and reducing the volume of the gearbox.

Dong, J. Z. (2007) illustrated the influence of the optimization of main geometric parameters on the performance parameters of megawatt wind turbine gearbox. He used the complex method to solve the optimization model, and achieved the goal of equal strength optimization design.

CHAPTER3 MATHODOLOGY

3.1   Flow Chart

The whole project process is shown in Figure 3.1.

```
                              ┌──────────────┐
                              │    Start     │
                              └──────────────┘
```

Start

Shigley's design method

• Shigley's design method is used to calculate safety factor of gears;

• Shigley's design method is used to calculate safety factor of shafts;

• Shigley's design method is used to calculate safety factor of keys;

• Shigley's design method is used to calculate the rated dynamic load of bearing.

Model Development

• Preliminary design model by UGNX software;

• Simplification of geometric model;

• Export models to ANSYS Workbench software.

Computational Analysis

• Analysis using ANSYS Workbench software;

• Static analysis;

• Fatigue failure analysis.

• Dynamic analysis (Modal analysis);

Design Optimization

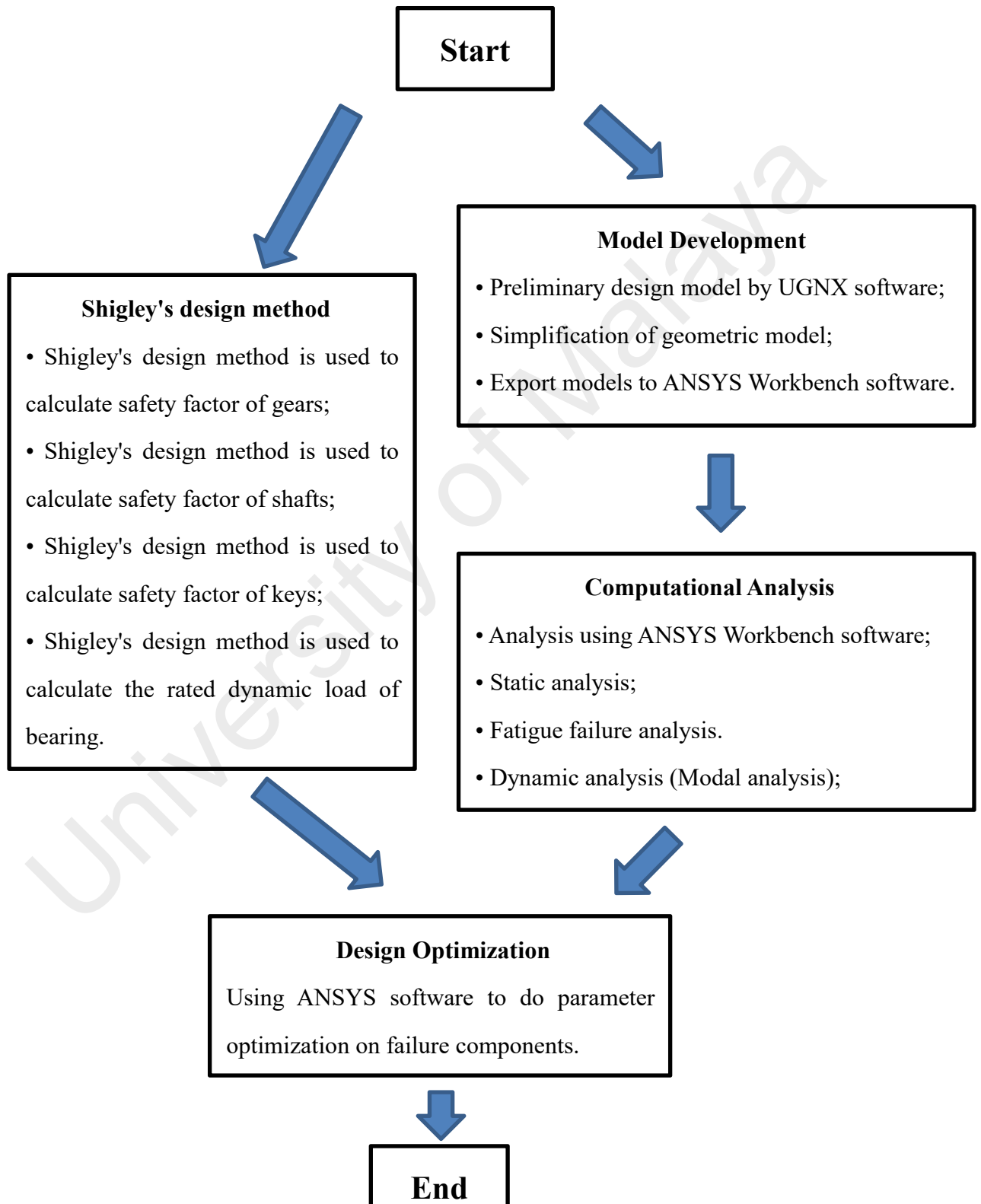Using ANSYS software to do parameter optimization on failure components.

End

Figure 3.1: Flow chart of the whole research process.

3.2 Statement of Methodology

The factor of safety is the coefficient used to reflect the structural safety degree in the engineering structure design method. Factor of safety involves the economic benefits of the project and the possible consequences of structural damage. If the factor of safety of the machine does not meet the standard (safety factor < 1.2), this machine may be damaged. Thus, in this chapter, the maximum stress, yield factor of safety and fatigue safety factor will be calculated to verify the reliability of each part of the speed increaser. Shigley's design method and computational analysis will be used to obtain stress and safety factor. The optimization methodology will be performed at the end of this chapter.

There are 6 gears and 3 shafts in this speed increaser gear box system. The structure of speed increaser is shown below on Figure 3.2:
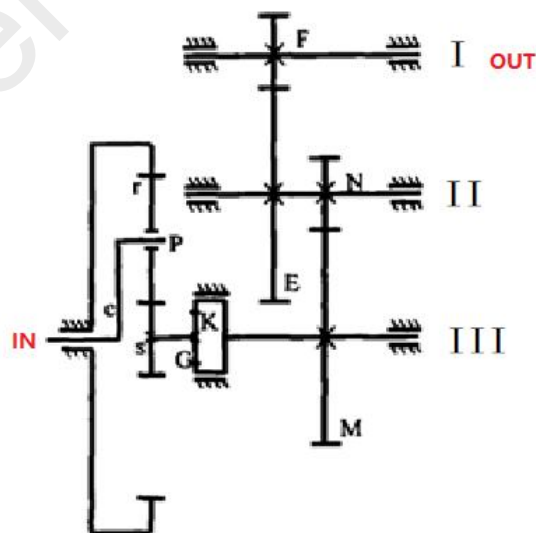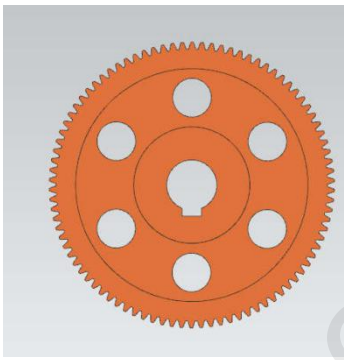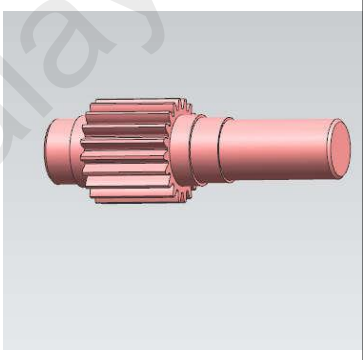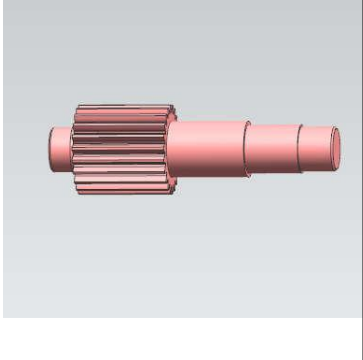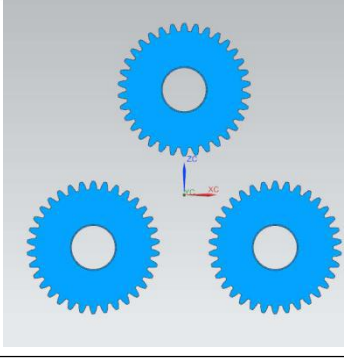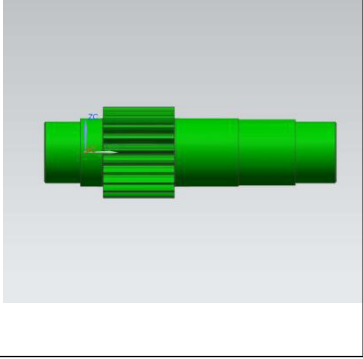

Figure 3.2: Structure of the speed increaser.

You can see it clearly in this figure that there 3 pairs of meshing gears and 3 shafts in this system. Meshing gears are gear E and F, gear M and N, gear P and S. In addition, shafts are shaft I, shaft II and shaft III. More parameters has been shown in chapter 2. The models of each component are shown below on Table 3.1. Next, these components will be calculated separately.

Table 3.1: Models of components of speed increaser.

Component	Model	Component	Model
Gear E		Gear F and Shaft I	
Gear M		Gear N and Shaft II	
Gear P		Gear S and Shaft III	

3.3 Shigley's design method

3.3.1 Calculation of Gears

The transmission parameters of gears and the details of each gear are shown below on the Table 3.2. Some original parameters has described in chapter 2. More calculation details are shown on APPENDIX. (A1 and A2)

Total gears transmission ratio: $e_{total} = \frac{1}{75}$

Gears transmission ratio between gear E and F: $\frac{N_F}{N_E} = \frac{1}{4.5}$

Gears transmission ratio between gear M and N: $\frac{N_N}{N_M} = \frac{1}{4.3}$

Gears transmission ratio between gear R and S: $\frac{N_S}{N_R} = \frac{1}{3.9}$

Table 3.2: Parameters of gears.

Gear	Number of teeth	Modules (teeth/in)	Pressure angle	Velocity (rev/min)	Thickness (mm)	Moment (N.m)	Geometry factor J	Life cycle	Material
F	20	2.11	20	1500	150	9549	0.33	1.57E+10	42CrMo
E	90	2.11	20	335	150	42970	0.43	3.5E+9	42CrMo
N	22	1.59	20	335	250	42970	0.33	3.5E+9	42CrMo
M	94	1.59	20	78	250	183600	0.43	8.1E+8	42CrMo
S	23	1.59	20	78	300	183600	0.33	8.1E+8	42CrMo
P	34	1.59	20	0	300	-	0.38	-	42CrMo

In the speed increaser, there are three pairs of meshing gears. In order to analyze the safety factor of each gear simply and accurately, each pair of meshing gears will be analyzed separately. Torque, power and speed of each pair of meshing gears will be added to the active wheels separately, and the safety factor of the gears will be

calculated by using AGMA design standard. Therefore we can use the formula mentioned in the chapter 2 to calculate the desired parameters.

Also, to calculate gears bending endurance strength safety factor and pitting safety factor, two parameters about gears material need to be introduced. They are allowable bending stress number S_t and allowable contact stress number S_c. They have been introduced on Table 2.3 in chapter 2. For ease of use, the two parameters are shown again below on the Table 3.3.

Table 3.3: allowable bending stress number & allowable contact stress number.

Material	allowable bending stress number S_t, (MPa)	allowable contact stress number S_c ,(MPa)
42CrMo	900	1650

In order to calculate the safety factor of gear, gear bending stress σ and gear contact stress σ_c need to be calculated first. We can find the relevant formula in the theory of chapter 2. From Equation 2.4 and Equation 2.11, the gear bending stress σ and the gear contact wear stress σ_c can be calculated respectively. Then we can use Equation 2.10 and Equation 2.15 to calculate gear bending safety factor S_F and gear pitting safety factor S_H, respectively. Factor of safety is a good index to identify failure of parts during work when S_F and S_H < 1.2.

The Shigley's design method of 3 pairs meshing gears are shown below:

1. Gear E and gear F.

From Equation 2.4, the gear bending stress σ of gear E and F can be calculated,

$$\sigma_E = W^t K_0 K_v K_s \frac{P_d}{F} \frac{K_m K_B}{J}$$

$$= 17892(1)1.62(1.27)\frac{2.11}{6}\frac{1.32(1)}{0.43}$$

$$= 39738 \text{ psi } (275 \text{ MPa})$$

$$\sigma_F = W^t K_0 K_v K_s \frac{P_d}{F} \frac{K_m K_B}{J}$$

$$= 17892(1)1.62(1.22)\frac{2.11}{6}\frac{1.32(1)}{0.33}$$

$$= 48111 \text{ psi } (330 \text{ MPa})$$

From Equation 2.10, the bending factor of safety S_F can be calculated,

$$S_{F,E} = \frac{S_t Y_N/(K_T K_R)}{\sigma}$$

$$= \frac{900(0.917)}{275}$$

$$= 3.0$$

$$S_{F,F} = \frac{S_t Y_N/(K_T K_R)}{\sigma}$$

$$= \frac{900(0.893)}{330}$$

$$= 2.4$$

From Equation 2.11, the gear contact wear stress σ_c can be calculated,

$$\sigma_{c,E} = C_p (W^t K_0 K_v K_s \frac{K_m}{d_p F} \frac{C_f}{I})^{1/2}$$

$$= 2276\left[17892(1)1.62(1.27)\frac{1.32}{42.5(6)}\frac{1}{0.131}\right]^{\frac{1}{2}}$$

$$= 86805 \text{ psi } (600 \text{ MPa})$$

$$\sigma_{c,F} = C_p(W^t K_0 K_v K_s \frac{K_m}{d_p F} \frac{C_f}{I})^{1/2}$$

$$= 2276\left[17892(1)1.62(1.22)\frac{1.32}{9.48(6)}\frac{1}{0.131}\right]^{\frac{1}{2}}$$

$$= 180880 \text{ psi } (1200 \text{ MPa})$$

From Equation 2.15, the gear pitting factor of safety S_H can be calculated,

$$S_{H,E} = \frac{S_C Z_N C_H/(K_T K_R)}{\sigma_c}$$

$$= \frac{1650(0.874)}{600}$$

$$= 2.4$$

$$S_{H,F} = \frac{S_C Z_N C_H/(K_T K_R)}{\sigma_c}$$

$$= \frac{1650(0.844)}{1200}$$

$$= 1.2$$

2. Gear M and gear N.

From Equation 2.4, the gear bending stress σ of gear M and N can be calculated,

$$\sigma_M = W^t K_0 K_v K_s \frac{P_d}{F} \frac{K_m K_B}{J}$$

$$= 54647(1)1.36(1.28)\frac{1.59}{10}\frac{1.479(1)}{0.43}$$

$$= 52025 \text{ psi } (358 \text{ MPa})$$

$$\sigma_N = W^t K_0 K_v K_s \frac{P_d}{F} \frac{K_m K_B}{J}$$

$$= 17892(1)1.36(1.27)\frac{1.59}{10}\frac{1.479(1)}{0.33}$$

$$= 67260 \text{ psi } (464 \text{ MPa})$$

34

From Equation 2.10, the bending factor of safety S_F can be calculated,

$$S_{F,M} = \frac{S_t Y_N / (K_T K_R)}{\sigma}$$

$$= \frac{900(0.941)}{358}$$

$$= 2.4$$

$$S_{F,N} = \frac{S_t Y_N / (K_T K_R)}{\sigma}$$

$$= \frac{900(0.0.917)}{464}$$

$$= 1.78$$

From Equation 2.11, the gear contact wear stress σ_c can be calculated,

$$\sigma_{c,M} = C_p \left(W^t K_0 K_v K_s \frac{K_m}{d_p F} \frac{C_f}{I} \right)^{1/2}$$

$$= 2276 \left[54647(1)1.36(1.28) \frac{1.479}{59.2(10)} \frac{1}{0.130} \right]^{\frac{1}{2}}$$

$$= 97315 \text{ psi } (670 \text{ MPa})$$

$$\sigma_{c,N} = C_p \left(W^t K_0 K_v K_s \frac{K_m}{d_p F} \frac{C_f}{I} \right)^{1/2}$$

$$= 2276 \left[54647(1)1.36(1.27) \frac{1.479}{13.85(10)} \frac{1}{0.130} \right]^{\frac{1}{2}}$$

$$= 200000 \text{ psi } (1380 \text{ MPa})$$

From Equation 2.15, the gear pitting factor of safety S_H can be calculated,

$$S_{H,M} = \frac{S_C Z_N C_H / (K_T K_R)}{\sigma_c}$$

$$= \frac{1650(0.901)}{670}$$

$$= 2.2$$

$$S_{H,N} = \frac{S_C Z_N C_H / (K_T K_R)}{\sigma_c}$$

$$= \frac{1650(0.874)}{1380}$$

$$= 1.06$$

3. Gear P and gear S.

From Equation 2.4, the gear bending stress σ of gear S can be calculated,

$$\sigma_S = W^t K_0 K_v K_s \frac{P_d}{F} \frac{K_m K_B}{J}$$

$$= \frac{224310}{3}(1)1.187(1.29)\frac{1.59}{12}\frac{1.495(1)}{0.33}$$

$$= 68724 \text{ psi } (474 \text{ MPa})$$

From Equation 2.10, the bending factor of safety S_F can be calculated,

$$S_{F,S} = \frac{S_t Y_N / (K_T K_R)}{\sigma}$$

$$= \frac{900(0.941)}{474}$$

$$= 1.8$$

From Equation 2.11, the gear contact wear stress σ_c can be calculated,

$$\sigma_{c,S} = C_p (W^t K_0 K_v K_s \frac{K_m}{d_p F} \frac{C_f}{I})^{1/2}$$

$$= 2276 \left[\frac{224310}{3}(1)1.187(1.25)\frac{1.495}{14.49(12)}\frac{1}{0.128}\right]^{\frac{1}{2}}$$

$$= 196475 \text{ psi } (1350 \text{ MPa})$$

From Equation 2.15, the gear pitting factor of safety S_H can be calculated,

$$S_{H,S} = \frac{S_C Z_N C_H / (K_T K_R)}{\sigma_c}$$

$$= \frac{1650(0.901)}{1350}$$

$$= 1.1$$

More details of parameters of gears are shown on APPENDIX. (A1 and A2)

For gear P the parameter and dimension are similar with gear S. But the diameter of gear P is bigger than the diameter of gear S. Thus, the factor of safety of bending and pitting of gear P are larger than that of gear S. Also, both bending safety factor and pitting safety factor of gear S are above 1.2. Thus, in order to simplify the calculation procedure, it is assumed that bending safety factor and pitting safety factor of gear P are 2.0 and 1.3, respectively.

3.3.2 Calculation of Shafts

We can know from Figure 3.2 that there are 3 shafts in this gear box system and the safety factor of shafts need to be analyzed to ensure safety. For the load of shafts, because the gear diameters are known and structure locations of shafts are set, the shear-moment diagrams of shafts can be produced. Transmitted loads have been calculated by using parameters and equations mentioned in chapter 2, so the radial and axial loads transmitted through the gears can be determined. From summation of force and moments on each shaft, ground reaction forces at the bearing position can be determined. For rotating shafts, only the resultant magnitude is needed, so force components at bearings are summed as vectors. Shear force and bending moment diagrams are usually obtained in two planes, and then summed as vectors at any point of interest. But in this case, the tangential force is far greater than radial force, so in order to simplify the calculation difficulty, only tangential force is used to calculate. A torque

diagram should also be generated to clearly visualize the transfer of torque from an input component, through the shaft, and to an output component.
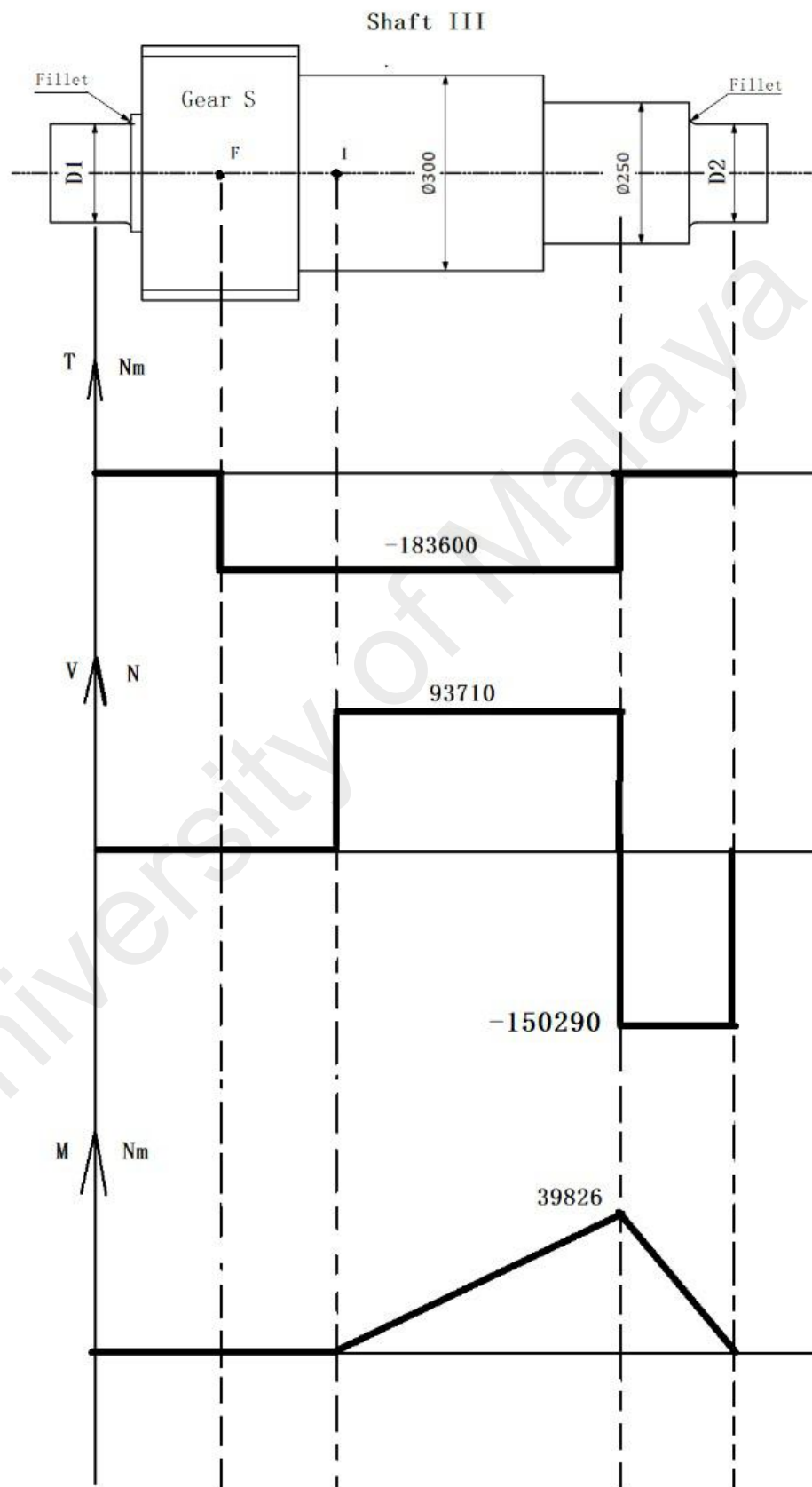

Figure 3.3: Shear-moment diagrams.

Here shaft III will be as an example to show the process of producing the shear-moment diagrams, shown on Figure 3.3. And other two diagrams are shown on APPENDIX, (A5). The material of shafts is 42CrMo, which property is shown on Table 2.2. The Tensile ultimate yield strength $S_{ut} = 1080\,\text{MPa}$. The Tensile yield strength $S_y = 930\,Mpa$. The safety factors of shafts will be determined based on Shigley's design method. The details of it are shown below.

The gears and bearings are located and supported by shoulders. The gears transmit torque through keys. The tangential force transmitted through the gears to shafts to be determined as follows. More details are shown on APPENDIX. (A3 and A4)

$$W_{MN}^t = 244000\,N$$

$$W_{EF}^t = 79582\,N$$

Now we have known W_{EF}^t and W_{MN}^t. Then the safety factor of shafts can be calculated easily by using Equation 2.16 to Equation 2.22 shown in Chapter 2. The safety factor of shafts includes the fatigue safety factor and yield safety factor of shoulders, the fatigue safety factor of keyway position and the fatigue safety factor of bearing position.

1. Shaft I

The maximum moment and torque of shaft I is $M_a = 17717$ Nm and $T_m = 9549$ Nm, respectively. (APPENDIX, A5)

From Equation 2.18,

$$S_e = k_a k_b k_c k_d k_e k_f S_e'$$

$$= 0.708(0.71)0.5(1080)$$

$$= 272 \text{ MPa}$$

From Equation 2.16 and 2.17,

$$\sigma_a = \frac{32 K_f M_a}{\pi d^3} = \frac{32(1.7)17717}{3.14(0.12)^3} = 177 \text{ } MPa$$

$$\sigma_m = \sqrt{3}\frac{16 K_{fs} T_m}{\pi d^3} = \sqrt{3}\frac{16(1.5)9549}{\pi 0.12^3} = 73 \text{ } MPa$$

From Equation 2.21 and 2.22,

Fatigue failure safety factor based on Goodman theory,

$$\frac{1}{n_f} = \frac{\sigma_a}{S_e} + \frac{\sigma_m}{S_{ut}} = \frac{177}{272} + \frac{73}{1080} = 0.5$$

$$n_f = 2.0 \text{ } (on \text{ } bearing \text{ } position)$$

Factor of safety of yielding,

$$n_y = \frac{S_y}{\sigma_a + \sigma_m} = \frac{930}{177+73} = 3.7 \text{ } (on \text{ } bearing \text{ } position)$$

2. Shaft II

The maximum moment and torque of shaft II is $M_a = 34627$ Nm and $T_m = 42970$

Nm, respectively. (APPENDIX, A5)

From Equation 2.18,

$$S_e = k_a k_b k_c k_d k_e k_f S_e'$$

$$= 0.708(0.69)0.5(1080)$$

$$= 267 \text{ MPa}$$

From Equation 2.16 and 2.17,

$$\sigma_a = \frac{32K_f M_a}{\pi d^3} = \frac{32(1.6)19174}{3.14(0.15)^3} = 93 \; MPa$$

$$\sigma_m = \sqrt{3} \frac{16K_{fs}T_m}{\pi d^3} = \sqrt{3} \frac{16(1.6)42970}{\pi 0.15^3} = 152 \; MPa$$

From Equation 2.21 and 2.22,

Fatigue failure safety factor based on Goodman theory,

$$\frac{1}{n_f} = \frac{\sigma_a}{S_e} + \frac{\sigma_m}{S_{ut}} = \frac{93}{267} + \frac{152}{1080} = 0.49$$

$$n_f = 2.0 \; (on \; gear \; shoulder \; position)$$

Factor of safety of yielding,

$$n_y = \frac{S_y}{\sigma_a + \sigma_m} = \frac{930}{93+152} = 3.7 \; (on \; gear \; shoulder \; position)$$

For the safety factor of key way position,

$$\sigma_a = \frac{32K_f M_a}{\pi d^3} = \frac{32(2.14)20000}{3.14(0.15)^3} = 129 \; MPa$$

$$\sigma_m = \sqrt{3} \frac{16K_{fs}T_m}{\pi d^3} = \sqrt{3} \frac{16(3.0)42970}{\pi 0.15^3} = 337 \; MPa$$

$$\frac{1}{n_f} = \frac{\sigma_a}{S_e} + \frac{\sigma_m}{S_{ut}} = \frac{129}{267} + \frac{337}{1080} = 0.8$$

$$n_f = 1.26 \; (on \; key \; way \; position)$$

For the safety factor of bearing position,

Because the moment is very small at bearing position, only need to consider bending

stress.

$$\sigma_a = \frac{32K_f M_a}{\pi d^3} = \frac{32(2.14)8000}{3.14(0.135)^3} = 90 \; MPa$$

$$n_f = \frac{S_e}{\sigma_a} = \frac{267}{90} = 2.9 \ (on \ bearing \ position)$$

3. Shaft III

The maximum moment and torque of shaft III is $M_a = 39826$ Nm and $T_m = 183600$

Nm, respectively. (APPENDIX, A5)

From Equation 2.18,

$$S_e = k_a k_b k_c k_d k_e k_f S_e^{'}$$

$$= 0.708(0.65)0.5(1080)$$

$$= 250 \ \text{MPa}$$

From Equation 2.16 and 2.17,

$$\sigma_a = \frac{32 K_f M_a}{\pi d^3} = \frac{32(1.6)23428}{3.14(0.21)^3} = 41 \ MPa$$

$$\sigma_m = \sqrt{3} \frac{16 K_{fs} T_m}{\pi d^3} = \sqrt{3} \frac{16(1.35)183600}{\pi 0.21^3} = 236 \ MPa$$

From Equation 2.21 and 2.22,

Fatigue failure safety factor based on Goodman theory,

$$\frac{1}{n_f} = \frac{\sigma_a}{S_e} + \frac{\sigma_m}{S_{ut}} = \frac{41}{250} + \frac{236}{1080} = 0.383$$

$$n_f = 2.6 \ (on \ gear \ shoulder \ position)$$

Factor of safety of yielding,

$$n_y = \frac{S_y}{\sigma_a + \sigma_m} = \frac{930}{41 + 250} = 3.3 \ (on \ gear \ shoulder \ position)$$

For the safety factor of key way position,

$$\sigma_a = \frac{32 K_f M_a}{\pi d^3} = \frac{32(2.14)39826}{3.14(0.21)^3} = 94 \ MPa$$

$$\sigma_m = \sqrt{3} \frac{16 K_{fs} T_m}{\pi d^3} = \sqrt{3} \frac{16(3.0)183600}{\pi 0.21^3} = 520 \ MPa$$

$$\frac{1}{n_f} = \frac{\sigma_a}{S_e} + \frac{\sigma_m}{S_{ut}} = \frac{94}{250} + \frac{520}{1080} = 0.85$$

$$n_f = 1.2 \ (on \ key \ way \ position)$$

For the safety factor of bearing position,

Because the moment is very small at bearing position, only need to consider bending stress.

$$\sigma_a = \frac{32K_f M_a}{\pi d^3} = \frac{32(2.7)6000}{3.14(0.12)^3} = 95 \ MPa$$

$$n_f = \frac{S_e}{\sigma_a} = \frac{250}{95} = 2.6 \ (on \ bearing \ position)$$

More details of parameters of shafts are shown on APPENDIX, (A3 and A4).

3.3.3 Calculation of Keys

Keys are used on shafts to secure rotating gears. For this speed increaser, the material of keys is 42CrMo and the property is shown on Table 2.2. There are 2 keys in this speed increaser: key II and key III.

Key II is used on shaft II connecting gear E & key III is used on shaft III connecting gear M. Keys are square key. The parameter is shown below on Table 3.4. And the models of keys are shown on Figure 3.4.

Table 3.4: Parameter of keys

	Key II	Key III
Width (mm)	50	57.2
Height (mm)	50.8	50.8
Length (mm)	80	140
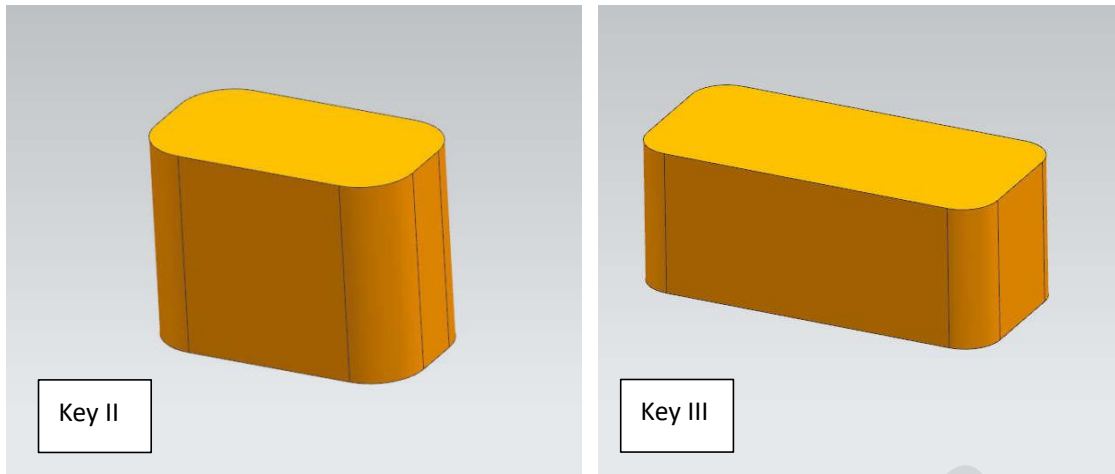
Figure 3.4: Models of keys.

1. Key II

The diameter of shaft II for key is 180mm; torque is 42972 Nm; rotating speed is 355 rev/min; shear force is 477445 N.

By the distortion-energy theory, the shear strength is:

$$S_{sy} = 0.577\, S_y = 0.577(930) = 536.61\, MPa$$

From Equation 2.23 and 2.24, the yield safety factor is,

$$\frac{S_{sy}}{n} = \frac{F}{tl}$$

$$\frac{536.6 \times 10^6}{n} = \frac{477445}{0.05 \times 0.07}$$

$$n = 3.9$$

To resist crushing, the area of one-half the face of the key is used:

$$\frac{S_y}{n} = \frac{F}{tl/2}$$

$$\frac{930 \times 10^6}{n} = \frac{477445}{0.05 \times 0.035}$$

$$n = 3.4$$

2. Key III

The diameter of shaft III for key is 290mm; torque is 183600 Nm; rotating speed is 78 rev/min; shear force is 1266206 N.

By the distortion-energy theory, the shear strength is:

$$S_{sy} = 0.577\,S_y = 0.577(930) = 536.61\,MPa$$

From Equation 2.23 and 2.24, the yield safety factor is,

$$\frac{S_{sy}}{n} = \frac{F}{tl}$$

$$\frac{536.6 \times 10^6}{n} = \frac{1266206}{0.0572 \times 0.14}$$

$$n = 3.3$$

To resist crushing, the area of one-half the face of the key is used:

$$\frac{S_y}{n} = \frac{F}{tl/2}$$

$$\frac{930 \times 10^6}{n} = \frac{1266206}{0.0572 \times 0.07}$$

$$n = 2.9$$

3.3.4   Calculation of Bearing

Since the bearings on these three shafts are same, the speed increaser adopts bearings of uniform specifications. In order to verify the safety of bearings at maximum load and maximum speed, we choose the bearing that installed on the fastest shaft and bearing maximum radial force. For this bearing, the maximum radial force is 197870 N, which can be calculated by using parameters in chapter 2. And the fastest speed of shaft is 1500 rev/min. Also, the design lift of this bearing is 3.5×10^9 cycles. Therefore, by calculating the rated dynamic load on this bearing , if the result is less than the basic rated dynamic load of the selected bearing within maximum radial force is 197870 N and rotating in 1500 rev/min, it means the bearing is safe.

The bearing is selected to SKF cylinder roller bearing that model is NUP 2324 ECML. By consulting the bearing parameters of SKF official network, the accurate parameters are obtained. The parameter of this bearing is show below on Table 3.5:

Table 3.5: Parameter of bearing.

Basic rated dynamic load	C	915	kN
Basic rated static load	C_0	1040	kN
Fatigue load limit	P_u	116	kN
Reference rotating speed		2800	rev/min
Limit rotating speed		5000	rev/min

We can see from the Table, reference rotating speed and limit rotating speed are all above the maximum rotating shaft speed 1500 rev/min, which means the bearing meets the speed requirements of all shafts of the speed increaser.

Next, we need to verify the rated dynamic load of bearings.

From Equation 2.25, the rated dynamic load on bearing can be calculated,

$$C_{10} = a_f F_D \left[\frac{x_D}{x_0 + (\theta - x_0)(1 - R_D)^{1/b}} \right]^{1/a}$$

$$C_{10} = 197870 \left[\frac{\frac{3.5 \times 10^9}{10^8}}{0.02 + 4.439(1 - 0.99)^{\frac{1}{1.483}}} \right]^{\frac{3}{10}} = 906 \, kN$$

Therefore, the basic rated dynamic load of SKF bearing is 915kN, which is greater than 906kN calculated and the reference rotating speed 2800 rev/min is also bigger than the highest speed of all three shafts 1500 rev/min. It means this bearing is safe.

3.4   Model Development

3.4.1   Preliminary Design of the Speed Increaser

The preliminary design of the speed increaser is produced by using UGNX software as shown below in Figure 3.5 and Figure 3.6. It consists of different parts like the casing of gear box, gears, shafts and bearings.
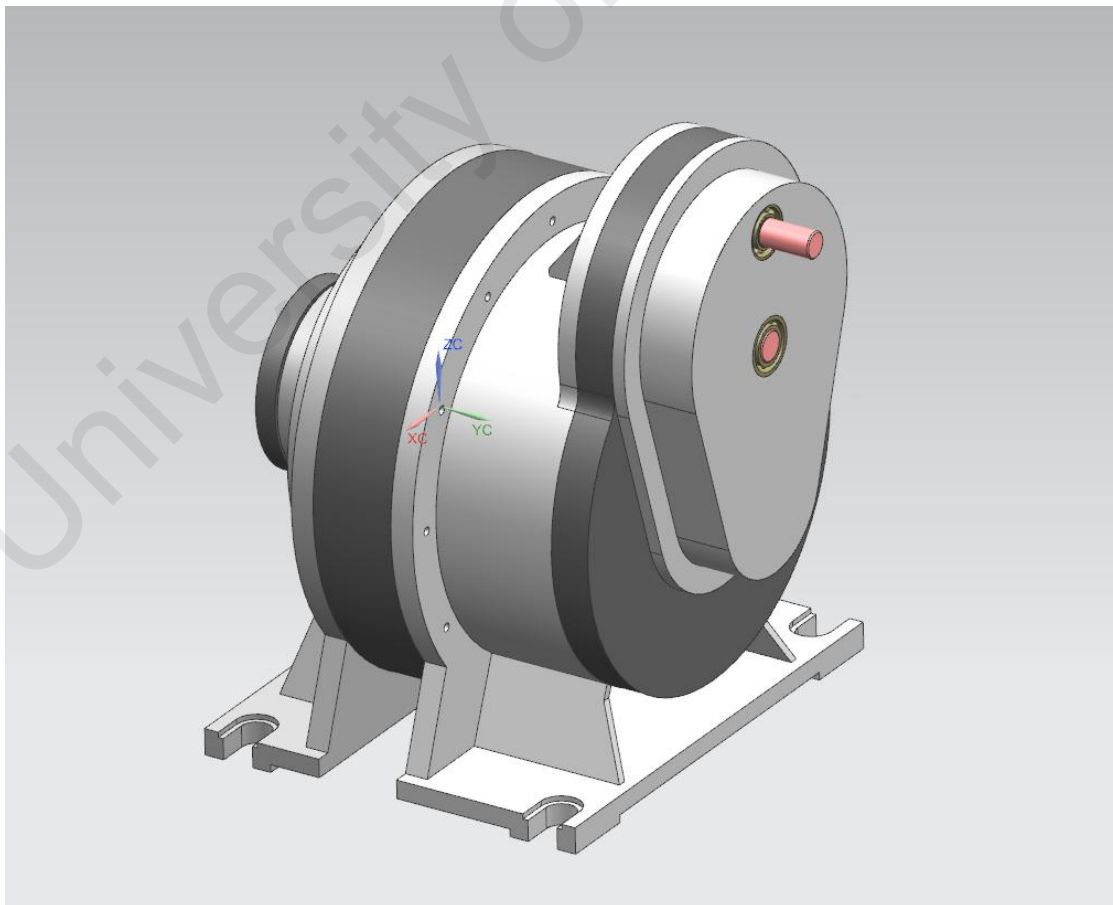
Figure 3.5: Casing of speed increaser.
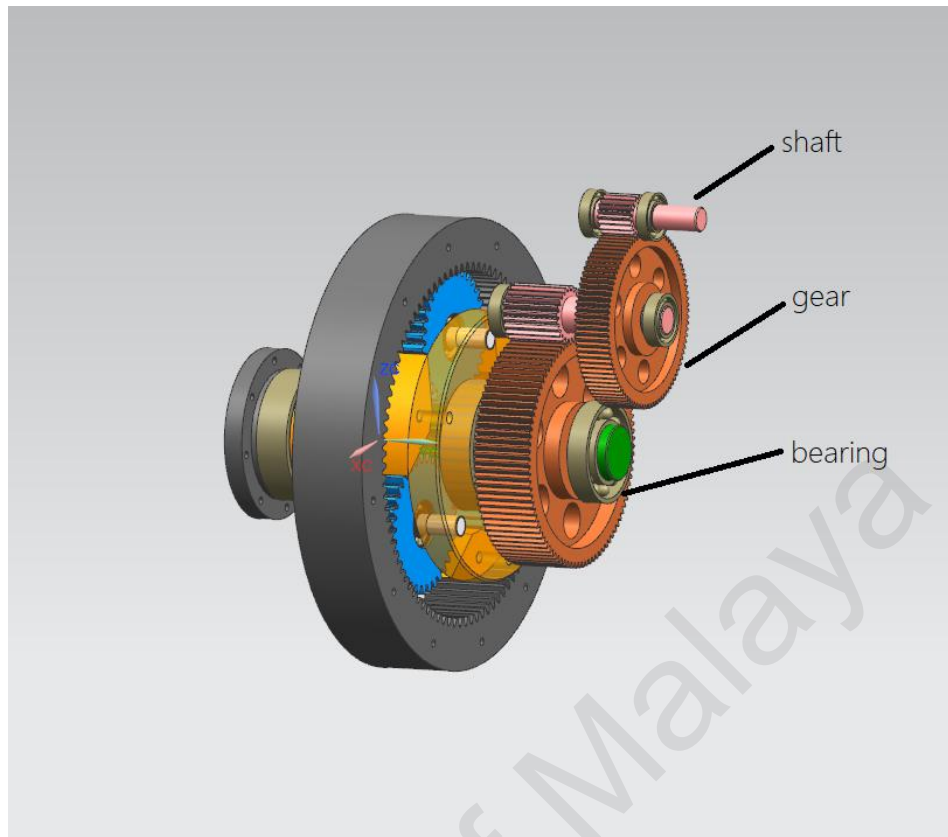
Figure 3.6: Gears, bearings and shafts of speed increaser.

3.4.2 Geometric Model for Analysis

When the speed increaser are static, each shaft has its own frequency. And then, when shafts are rotating, their speed will stabilize them at a specific frequencies. If these frequencies are consistent with the natural frequency of the gear shafts, resonance will occur, resulting in failure of parts. When the gear shafts are rotating, the frequency is easy to find by Equation 3.1.

$$\text{Frequency} = \frac{\omega}{60} \ \text{Hz} \qquad\qquad \text{Equation 3.1}$$

Where,

ω is the speed of shaft, rev/min

We have know the input speed (20 rev/min) and output speed (1500 rev/min) of speed increaser. Also, the transmission ratio of each stage gear is known, shown in chapter 3. We can easily get the rotating speed of each shaft.

Rotating speed of shaft I is 1500 rev/min;

Rotating speed of shaft II is 334 rev/min;

Rotating speed of shaft III is 78 rev/min;

From Equation 3.1, the rotating frequencies of shaft can be calculated and they are shown below on table 3.6.

Table 3.6: Rotating frequency of shafts.

	Rotating frequency
Shaft I	1.3 Hz
Shaft II	5.58 Hz
Shaft III	25 Hz

3.4.3 Simplification of Geometric Model

In finite element analysis, if we want to accurately calculate these features, we need to generate many small units, which will make the solution complex, time-consuming, and even fail. So it is important to simplify parts of speed increaser.

1. Simplification of Gear Shafts

In order to analyze gear shafts more concisely and effectively with finite element method, this project uses the method of deleting gear teeth and transforming them into

flat cylinders of the same weight. The result of before and after of simplification is shown in Figure 3.7.

Before   After
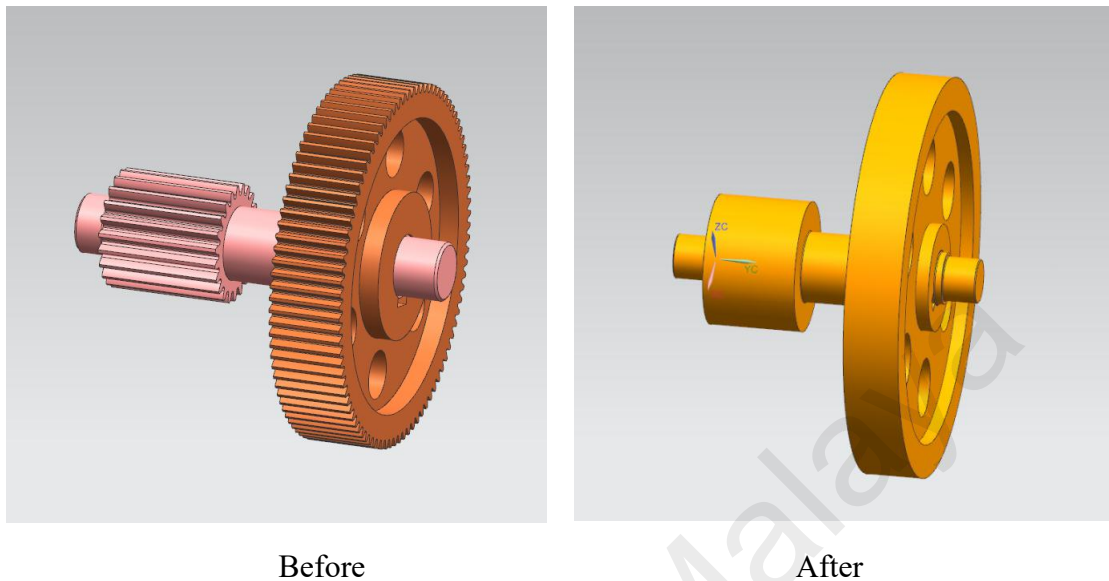
Figure 3.7: Simplification of gear shaft

2.   Simplification of Casing

For the finite element analysis of the casing, the main purpose is to analyze the deformation of the casing caused by the weight of the speed increaser. Thus, for simplification of casing, the method is that removes the gears, shafts and bearings in the casing, and adds a shaft of equal weight into casing, shown on Figure 3.8.

Before   After
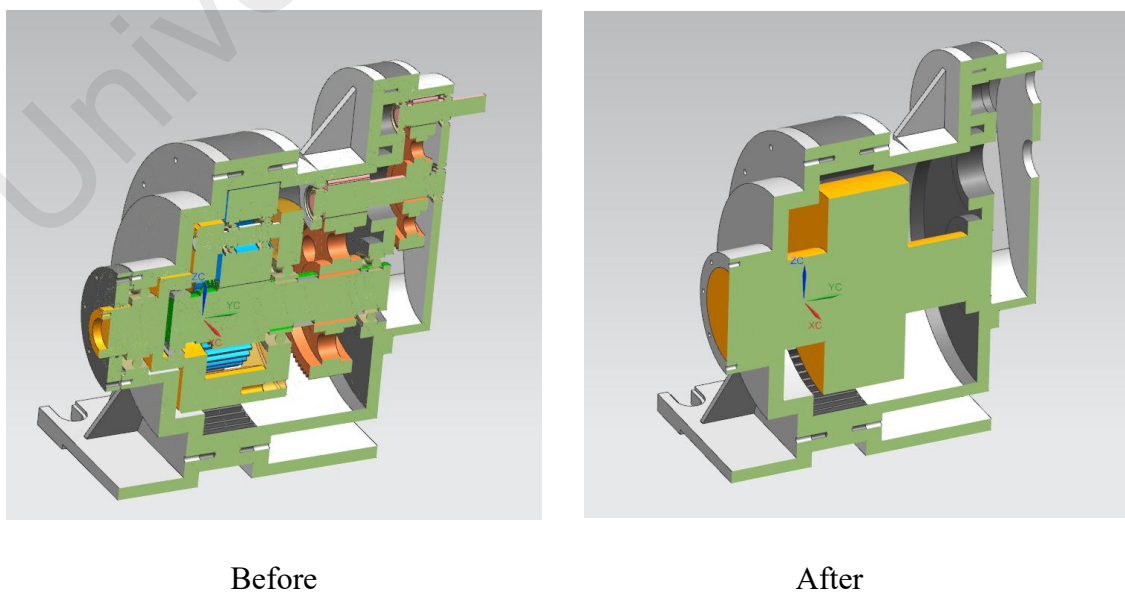
Figure 3.8: Simplification of casing

3.5   Computational Analysis

3.5.1   Static Analysis

The von Mises stress, strains and yield safety factor caused form external force can be measured by using static analysis method performed in ANSYS workbench software. The procedure and analysis are as follows:

1. Build model of gears, shafts, keys and bearing in UGNX software.

2. Run ANSYS Workbench 18.0 software.

3. Create static structural analysis system from the tool box.

4. Insert geometry into ANSYS.

5. Add material in Engineering Data (42CrMo or QT400), respectively.

6. Launch the mechanical model analysis system.

7. The connections of the geometry are set as bonded or no separation, respectively.

8. Meshing geometries.

9. Boundary condition is set for the fixed support where the place is fixed.

10. Boundary condition is set for the cylinder support where the place is supported by bearing.

11. Load applied is from the translation of gears (Force or Moment).

12. The results of static analysis will include:

    a. Total deformation,

    b. Equivalent stress (Equivalent Von-Mises Stress),

    c. Safety factor from stress tool (Max Equivalent Stress).

3.5.2 Fatigue Failure Analysis

The Fatigue failure safety factor caused by external force transformation can be measured by using fatigue failure analysis method performing in ANSYS software. The procedure and analysis are as follows:

Gears, shafts, keys and bearing will be analyzed the fatigue failure safety factor in ANSYS workbench 18.0 software.

1. The first to the tenth step are the same as the static analysis mentioned above.

2. The results of fatigue analysis will include:

a. Safety factor from fatigue failure tool.

3.5.3 Dynamic Analysis (Modal Analysis)

The natural frequency and mode from the characteristics of the structure of model can be found by using modal analysis method.

Gears, shafts, keys, bearing and casing will be analyzed on modal analysis in ANSYS workbench software.

The procedure and analysis are as follows:

1. Run ANSYS Workbench 18.0 software.

2. Create Modal analysis system from the tool box.

3. Geometry is added into ANSYS from UGNX file.

4. Add material in Engineering Data (42CrMo or QT400), respectively.

5. Launch the modal mechanical analysis system.

6. The connections of the geometry are set as bonded or no separation, respectively.

7. Meshing geometries.

8. Boundary condition is set for the fixed support where the place is fixed.

9. Boundary condition is set for the cylinder support where the place is supported by bearing.

10. First ten modes are inserted in analysis setting and the frequency at the range of interest is obtained.

11. The solution retrieved as:

    a. The magnitude of the first ten frequencies.

    b. Total deformation in these ten frequencies.

3.6   Design Optimization

The aim of optimization is to achieve reasonable effect and safety value by changing the length, width or size of geometric model. The procedure and analysis are as follows:

Optimization will be perform in ANSYS Workbench software.

1. Run ANSYS Workbench 18 software.

2. Create optimization system from the tool box.

3. Geometry is added into ANSYS.

4. Open the sketch editing interface.

5. In the project sketch, the parameter key "DS" is used to pre-set the geometric options to facilitate parameter selection.

6. Design variables are selected by clicking on the letter "p" in the box.

7. In the parameter set, the input parameters are selected and the output parameters need to be modified. They are length, width, diameters and safety factor.

8. In the experimental design, the design variables are set to upper and lower bounds. This topic uses DX to retain the key points of design after putting into production, and adopts the face-centered design method. Several design points will be generated.

9. On the response surface, the design points are retained after running with DX. At the response point, the response displays the 3D pattern in the outline: response attribute.

10. Insert goals and constraints in the optimization tab. The optimization method is screened out. Three of the best candidates will appear.

11. In the parameter set, the required parameters are copied to the current and updated to obtain a new parameter set.

CHAPTER 4: RESULTS AND DISCUSSION

4.1 Introduction

In this study, the components are analyzed based on two methods: (i) Shigley's design method and (ii) Computational analysis by using ANSYS Workbench 18.0 software. Through the analysis of these two methods, the safety factor of gears, shafts, bearings and casing of speed increaser will be calculated. The optimization will be performed on the parameter of components in ANSYS software.

The purpose of calculation is to effectively reflect the safety level of components. For finite analysis by ANSYS, the natural frequency and model shapes of the structures will be determined through modal analysis. Then, factor of safety from the fatigue tool and stress tool will be determined.

Optimization is carried out when the design of the model is likely to fail. Design of experiment, response surface and optimization is utilized to improve the design of the model. After the improved model is obtained, it will be re-analyzed again to ensure rationality.

4.2 Gears

The model of gears have been built by using UGNX software, which is shown below on Figure 4.1:
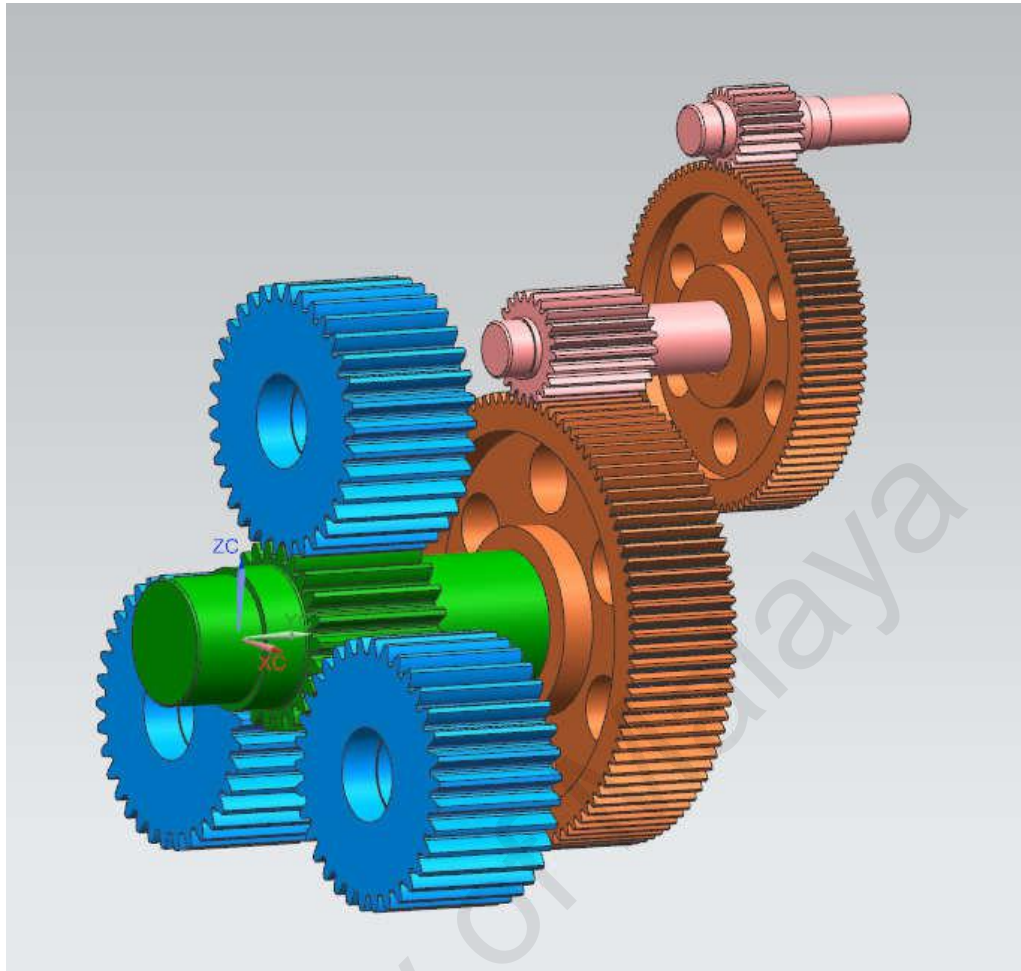
Figure 4.1: Models of gears.

4.2.1 Results of Shigley's design method

The calculation of safety factor of gears is carried out by using Equation 2.1 to Equation 2.10. From Figure 3.2, there are 3 pairs of meshing gears that need to be calculated can be known. They are gear E and F, gear M and N, gear S and P. The meshing process of gear P with gear R is similar to that of gear P with gear S. Here we can analyze the gear P only by using the meshing gears of P and S. After calculating the results of bending safety factor n and pitting safety factor n_c about 6 gears are shown below on the Table 4.1.

Table 4.1: Result of gears based on Shigley's design method.

Gears	Bending safety factor n	Wear safety factor n_c
Gear E	3.0	2.4
Gear F	2.4	1.2
Gear M	2.4	2.2
Gear N	1.78	1.06
Gear S	1.8	1.2
Gear P	2.0	1.3

As shown in the table, the safety factor of all gears are above 1.2 (safety factor > 1.2), which verifies that all gears can work safely within the design scope.

4.2.2   Results of Computational Analysis

The computational analysis using ANSYS Workbench 18.0 is an effective method to calculate the yield failure safety factor and fatigue failure safety factor of gears. And it can clearly show the damages of gears and position of the maximum stress and deformation, which is very effective for us to optimize the part if it has failure. Deformation of the gears, maximum equivalent stress and safe factor of the gears will be analyzed at below.

The material of gears is 42CrMo and the first step is meshing on gears. In next step the friction less support is applied on the hole of gears to simulate the shafts supporting gears. The third step is to set fixed support on bearing position of gear shaft, which can

simulate the gear shaft supported by bearing. Also, the gear ring is added fixed support to fix it on casing. The last step is to add moment on active gears.

The moment 42970 N · m, 183600 N · m and 61150 N · m are added to gear E, gear M and gear P, respectively. This step is shown on figure 4.2.
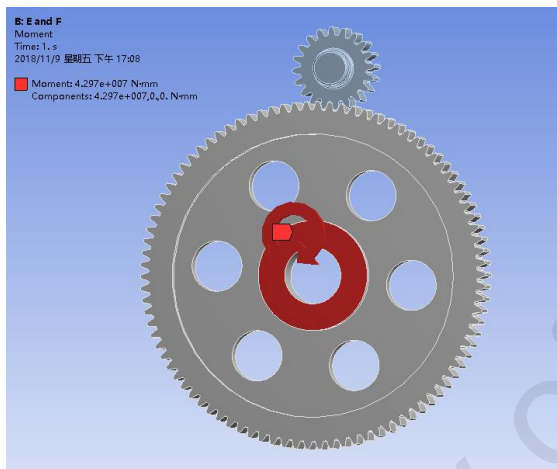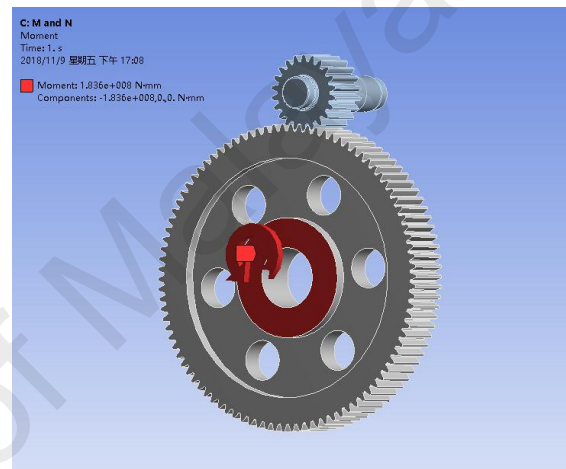
a). Gear E and gear F;   b). Gear M and gear N;
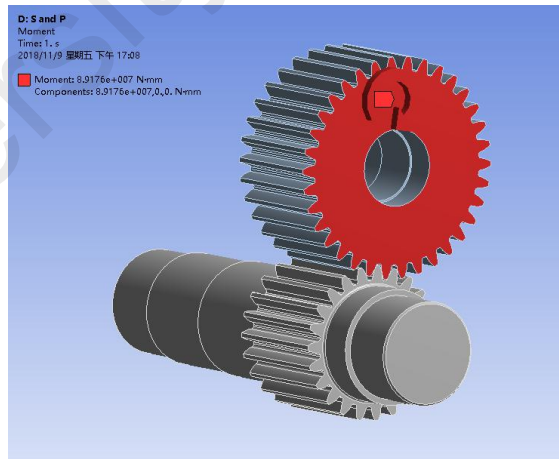
c). Gear S and gear P;
Figure 4.2: Moment added to the gears.

4.2.2.1 Static Analysis

The maximum stress obtained from the solution in ANSYS Workbench on these four coupling gears is 132.29 MPa (Figure 4.3, b), which is much lower than the yield strength of the material, and the maximum deformation is 0.89718 mm (figure 4.4, b). Also, the minimum safety factor of these 4 coupling gears obtained from the stress tool is 7.0302 (Figure 4.5, b). The details of result are shown on Figure 4.3 to Figure 4.5.

4.2.2.2 Fatigue Failure Analysis

The minimum safety factor from fatigue tool is 2.6533 (Figure 4.6, b). The details of result are shown on Figure 4.6.

Compared with the results of static analysis, there is no failure on gears. The details of computational analysis results of each pair of gears are show below on Table 4.2.

Table 4.2: The results of computational analysis of gears.

	Maximum Equivalent Stress (MPa)	Max Total Deformation (mm)	Safety factor of Yield Failure	Safety factor of Fatigue Failure
Gear E and F	46.391	0.039469	15.00	7.5662
Gear M and N	132.29	0.089718	7.0302	2.6533
Gear S and P	89.269	0.067346	10.418	3.9319

We can see from the Table, the maximum stresses of all gears are smaller than yield strength; maximum deformation is within the qualified range; safety factors are greater than 1.2.

a. Gear E and F

b. Gear M and N

c. Gear S and P
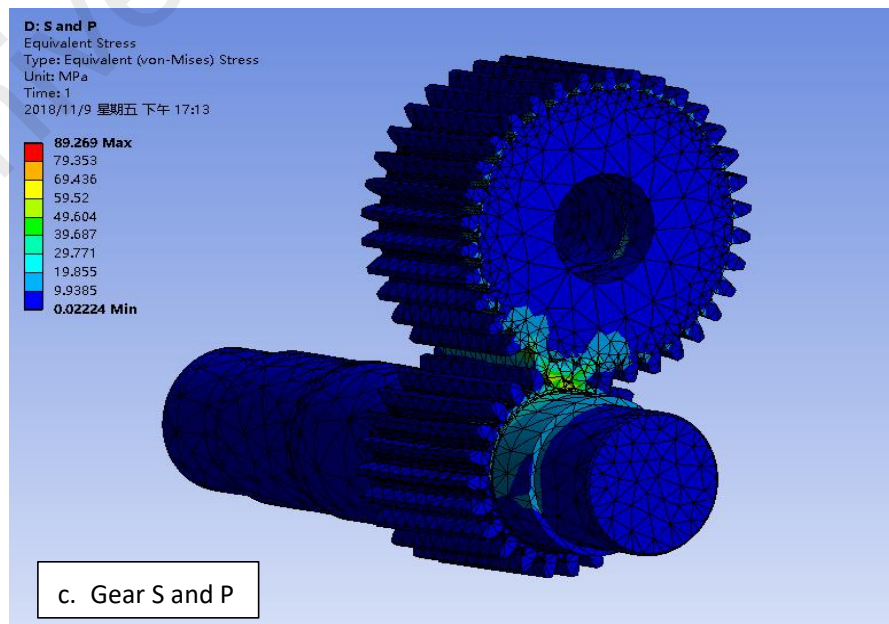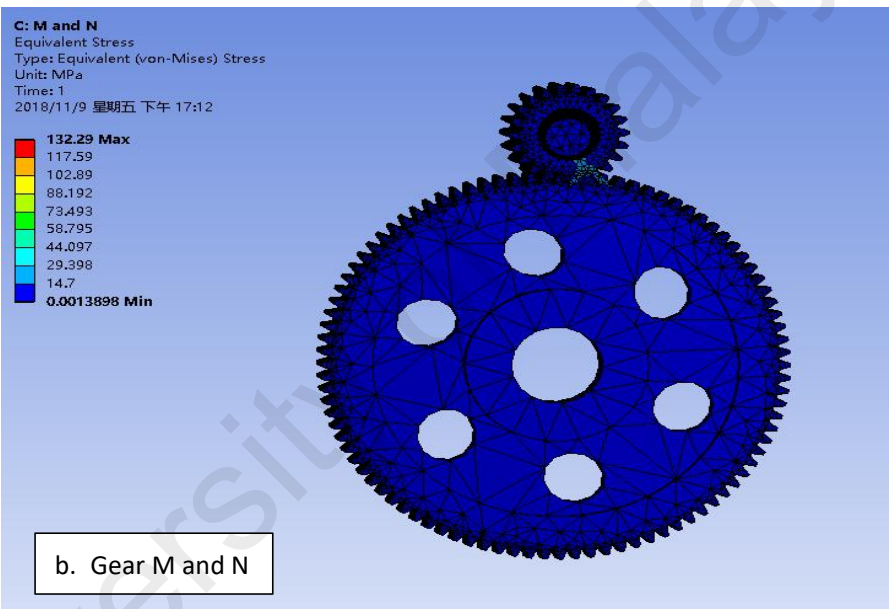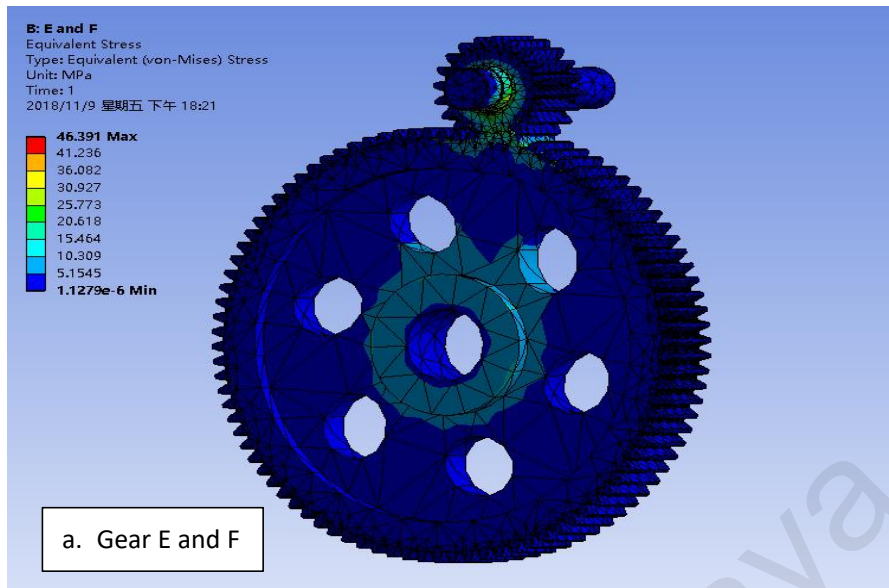
Figure 4.3: Maximum equivalent stress of the gears.
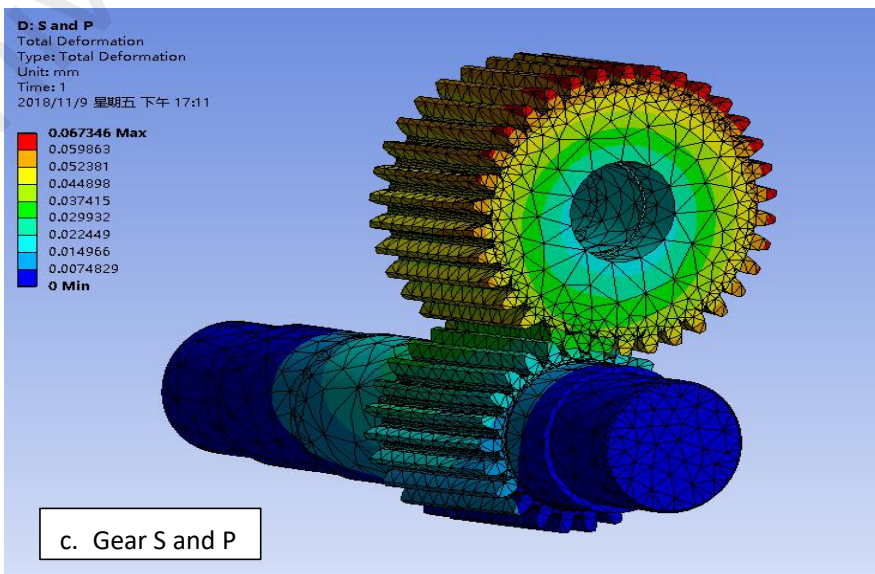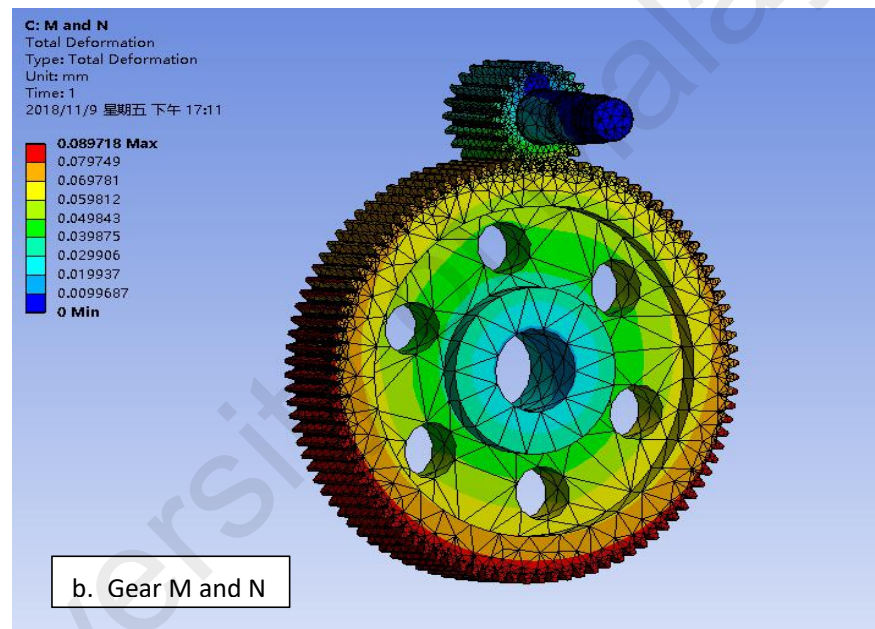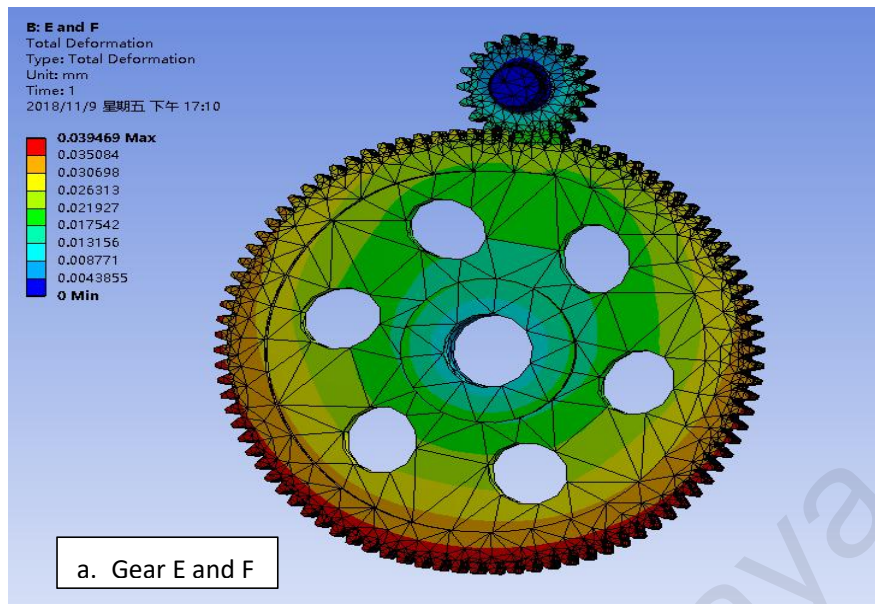
a. Gear E and F

b. Gear M and N

c. Gear S and P

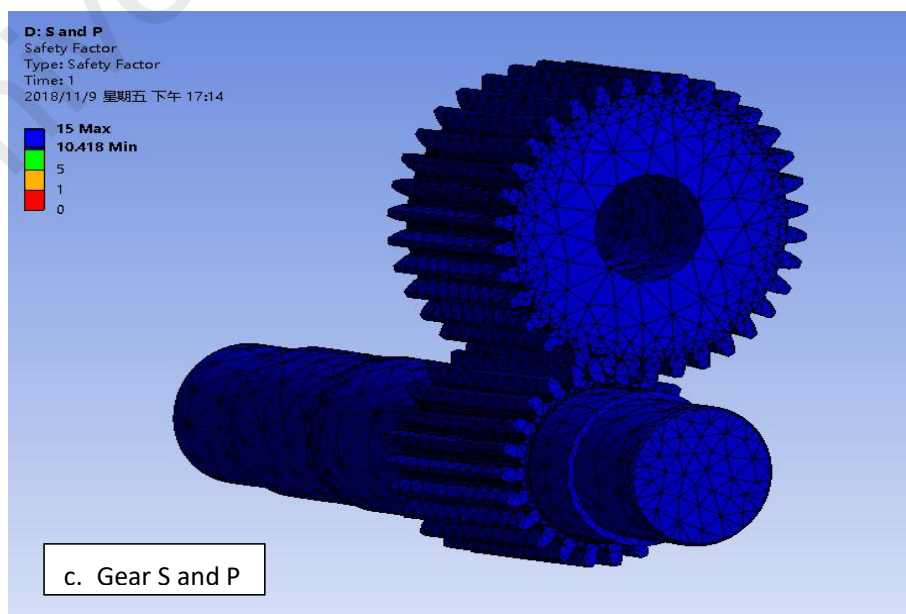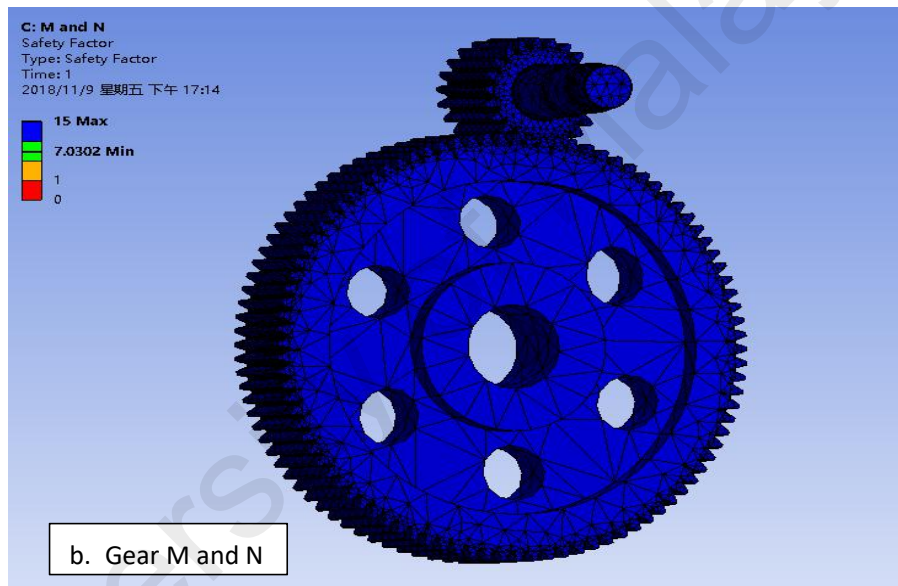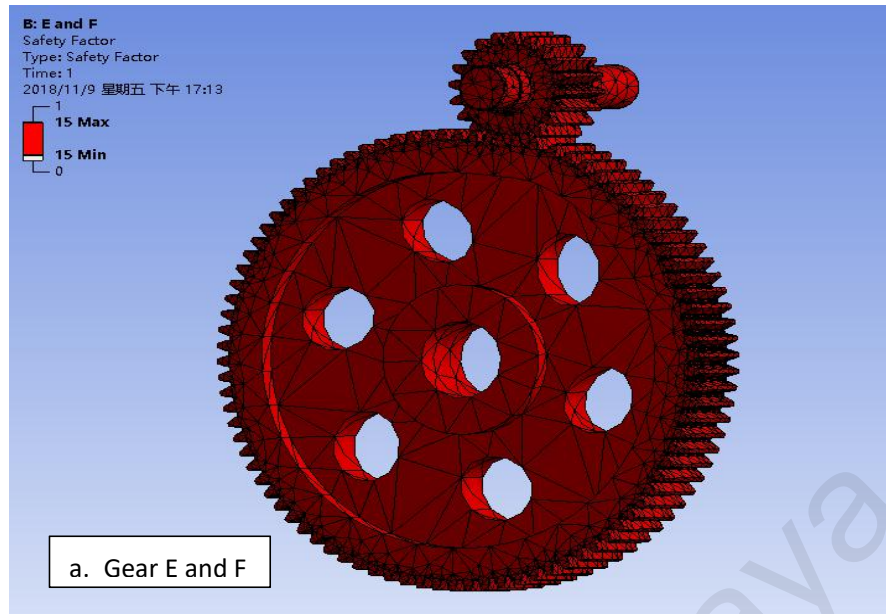Figure 4.4: Deformation of the gears.

a. Gear E and F

b. Gear M and N

c. Gear S and P

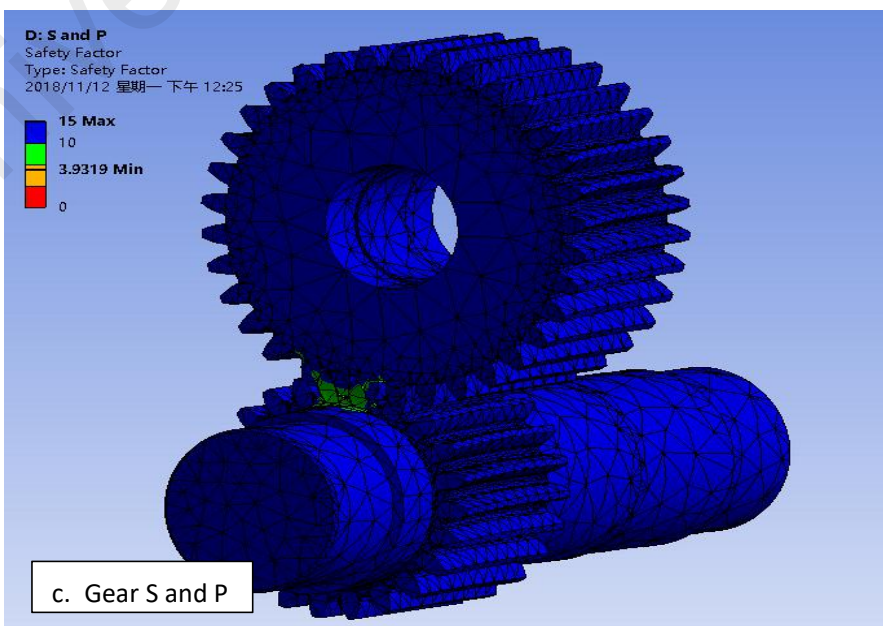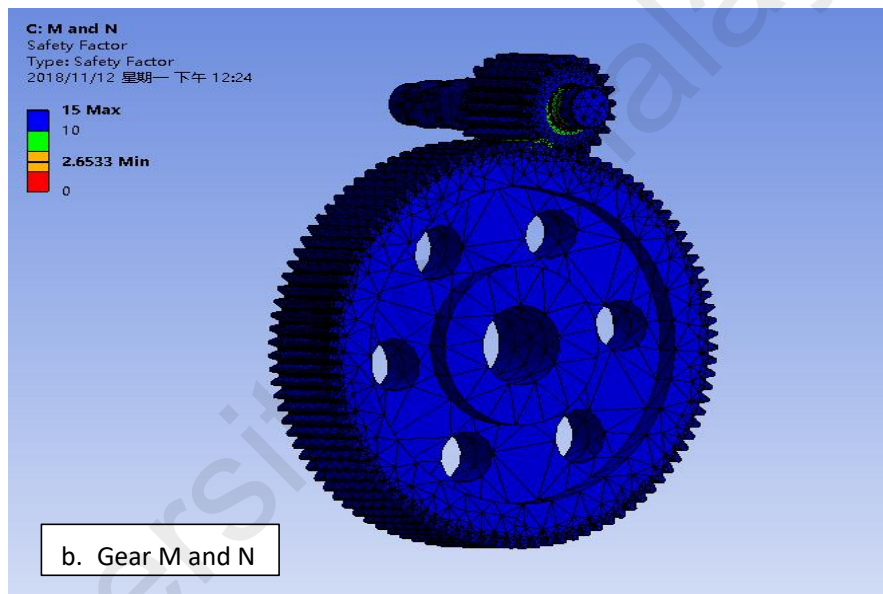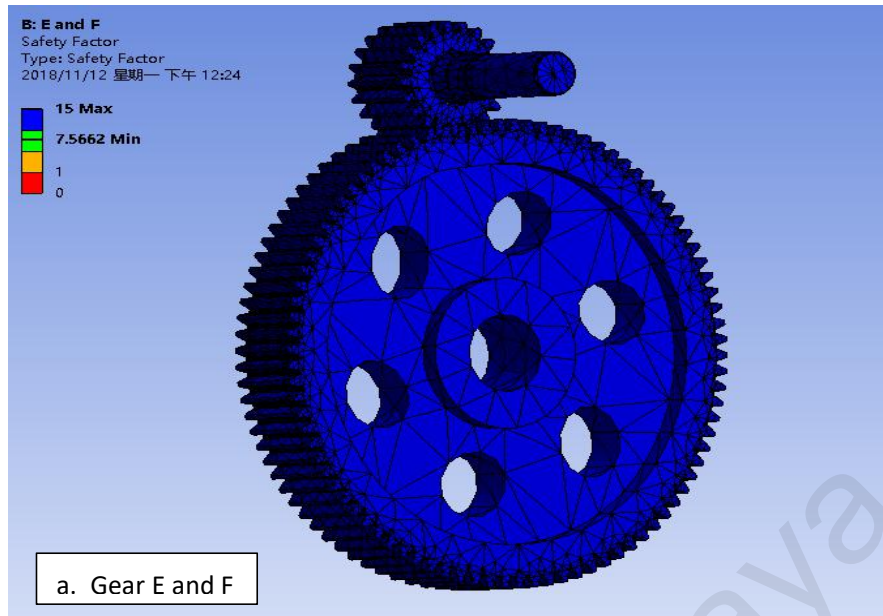Figure 4.5: Safe factor of the gears from the stress tool.
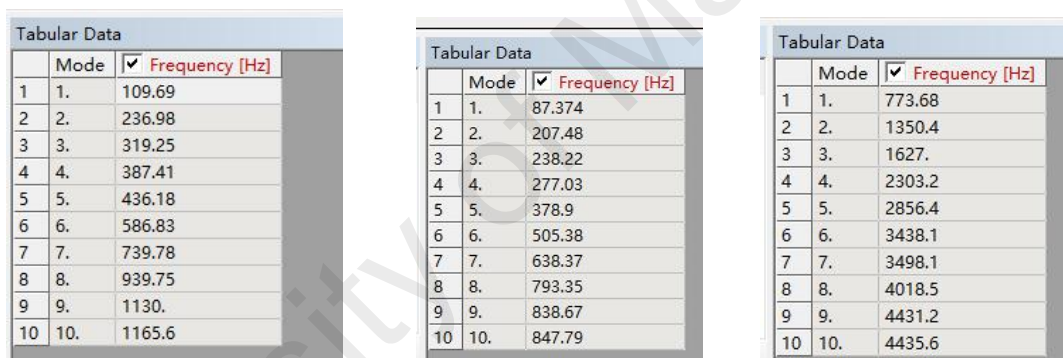
Figure 4.6: Safe factor of the gears from fatigue tool.

4.2.2.3 Modal Analysis

The purpose of modal analysis is to find the natural frequencies of gears and it can help to obtain the stresses above resonance. The results are calculated for the first 10 modes of each coupling gear and they are shown on Figure 4.7 below. In Figure 4.7, the minimum frequency of gears is 87.374 Hz. Reviewing chapter 3, the working frequencies of shafts were shown on Table 3.6. It shows that the highest rotating frequency is 25 Hz, which is lower than 87.374 Hz. Therefore, the resonance will not happen.

Gear E and F;　　　　　Gear M and N;　　　　　Gear P and S;

Figure 4.7: Modal analysis of natural frequency of gears.

4.2.3　Discussion

We have analyzed gears in two methods, Shigley's design method and computational analysis. Comparing the two methods, their results of safety factor are both above 1.2, which means that all gears are safe. But compared with the safety factor, the calculated safety factor is much smaller than the computer analyzed one. Compared with the maximum stress, the calculated stress is much larger than the computer analyzed one. The reasons for this difference may be:

1. Computational analysis is to analyze the whole gear: deformation and stress of integral gear above meshing force. However, the Shigley's design method is for the teeth of gears.

2. The Shigley's design method focuses more on the analysis of stress concentration failure of gear root and wear failure of tooth surface. Shigley's design method method is more detailed, which is the reason why the safety factor is less than that of computational analysis. Computational analysis is to analyze the whole gear, which includes the overall analysis of the entire gear. FEA method shows that when the whole gear is subjected to meshing force, the gear will not be damaged and fatigue wear.

4.3   Shafts

The model of gears have been built by using UGNX software, which is shown below:
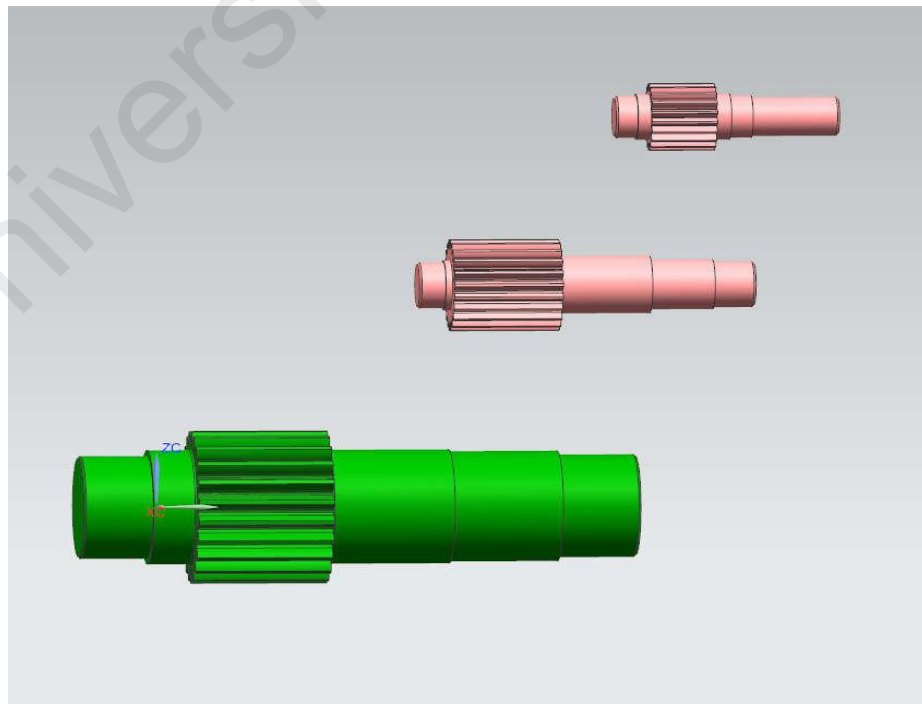

Figure 4.8: Models of shafts.

4.3.1 Results of Shigley's design method

The Shigley's design method of shafts is carried out by using Equation 2.16 to Equation 2.22. And from Figure 3.2 that there are 3 shafts need to be calculated can be known. They are shaft I, shaft II and shaft III. After calculating, the results of the fatigue safety factor n_f and the yield safety factor n_y of gear shoulder position, the fatigue safety factor n_f of keyway position and the fatigue safety factor n_f of bearing position about 3 shafts are shown below on the Table 4.3.

Table 4.3: Results of shafts based on Shigley's design method.

	Shaft I	Shaft II	Shaft III
Gear shoulder fatigue safety factor	-	2.0	2.6
Gear shoulder yield safety factor	-	3.7	3.3
Key way fatigue safety factor	-	1.26	1.2
Bearing position fatigue safety factor	2.0	2.9	2.6
Bearing position yield safety factor	3.7	> 2.9	> 2.6

As shown in the table, safety factor of all shafts are above 1.2 (safety factor > 1.2), which verifies that all shafts can work safely within the design scope. However, the key way position fatigue safety factor of shaft III is close 1 and it will also be analyzed by computational analysis.

4.3.2 Results of Computational Analysis

Firstly, the shafts need to be simplified using the method shown on Chapter 3. The yield safety factor and the fatigue safety factor of shafts will be analyzed in ANSYS.

Deformation of the shafts, maximum equivalent stress and safe factor of the shafts will be analyzed at below.

The material of shafts is 42CrMo and the first step is meshing on. In next step the cylindrical support is applied on the bearing position of shafts to simulate the supporting of bearings. The third step is to add forces on shafts. The forces can be calculated by using Equation 2.3 in chapter 2. The calculation process is omitted. The force 79580 N and 244000 N are added to gear E and F, gear M and N, respectively. And the force 36726N is added to the output of shaft. This step is shown below on Figure 4.9.
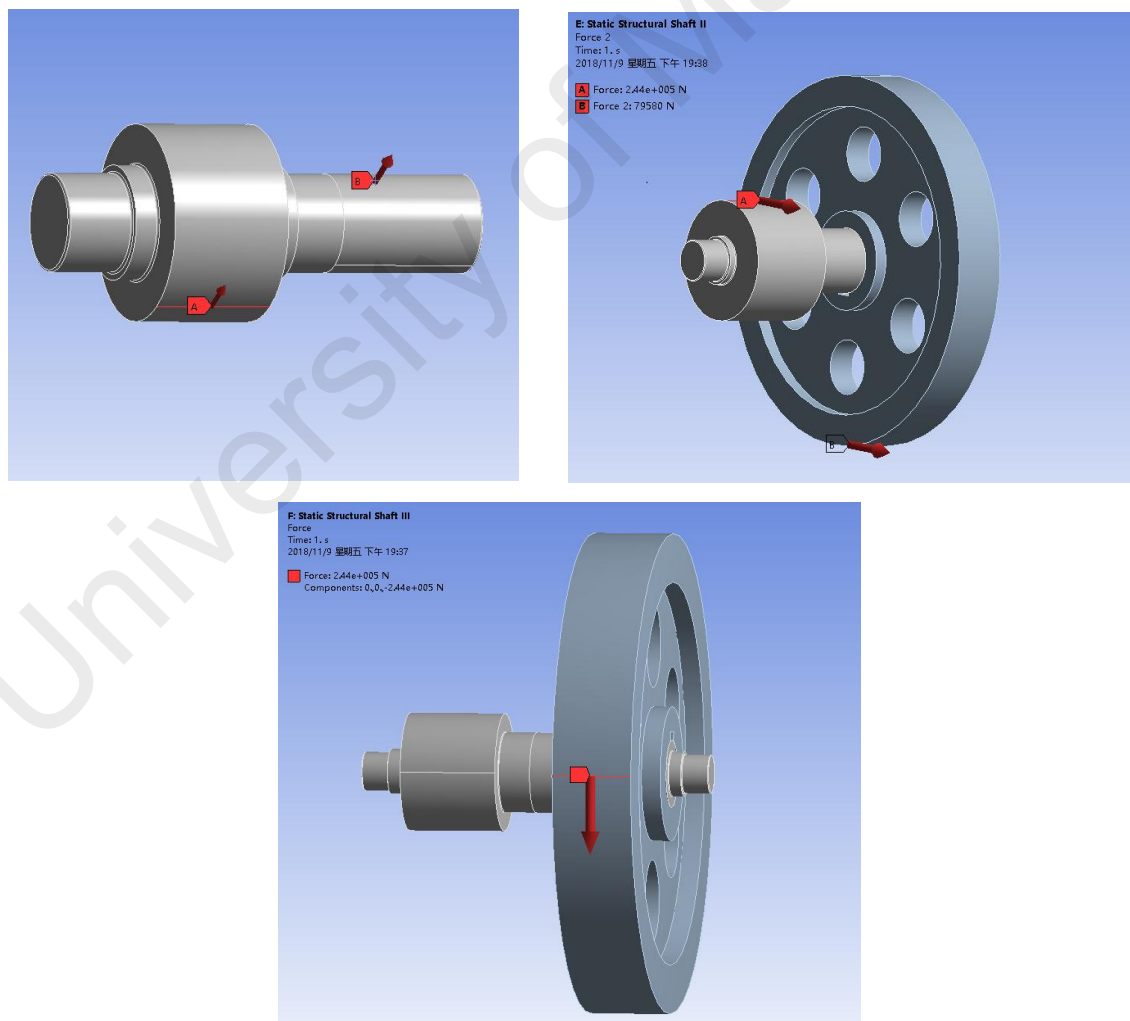

Figure 4.9: Force added to the shafts.

4.3.2.1 Static Analysis

The maximum stress obtained from the solution in ANSYS Workbench 18.0 on these three shafts is 1184.5 MPa (Figure 4.10, c), which is too large to fail. The maximum deformation is 0.26357 mm (figure 4.11, c). Also, the minimum safety factor of these 3 shafts obtained from the stress tool is 0.78517 (Figure 4.12, c). The details of three shafts are shown on Figure 4.10 to Figure 4.12.

4.3.2.2 Fatigue Failure Analysis

The minimum safety factor from fatigue tool is 0.32926 (Figure 4.13, c). The detail is shown on Figure4.13.

In summary, there is a failure on the shaft III. The problem is mainly concentrated on the bearing position and key way position of shaft III, because the biggest stress is focused on. Thus, the parameter of shafts needs to be optimized. The results of each shaft are shown below on Table 4.4.

Table 4.4: The results of computational analysis of shafts

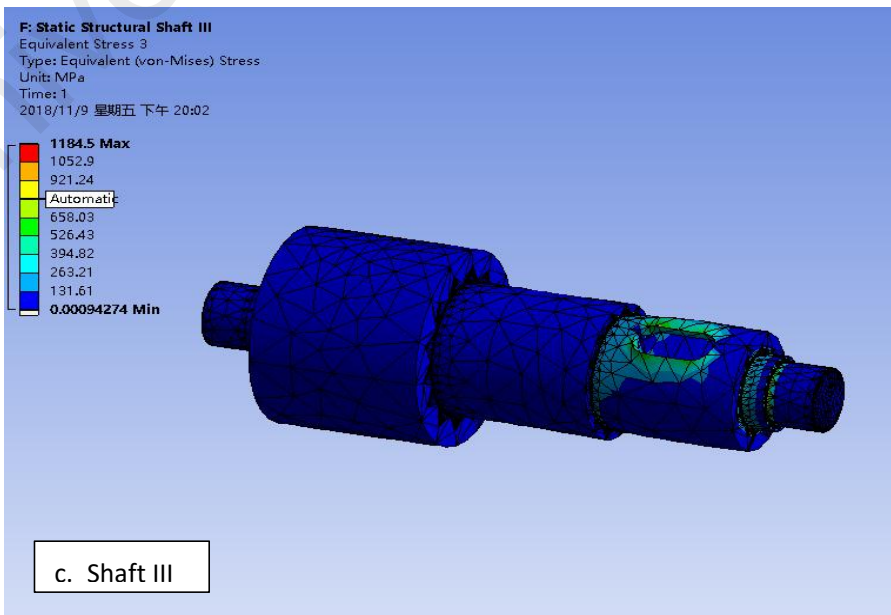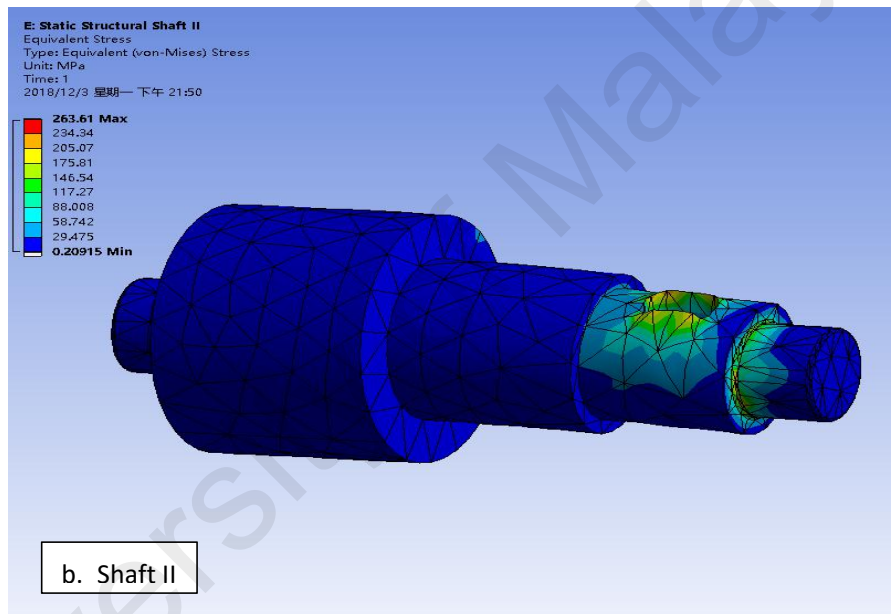|	Maximum Equivalent Stress (MPa)	Max Total Deformation (mm)	Safety factor of Yield Failure	Safety factor of Fatigue Failure
Shaft I	114.45	0.026736	8.126	3.0669
Shaft II	263.61	0.075271	3.528	1.3315
Shaft III	1184.5	0.26357	0.78517	0.32926

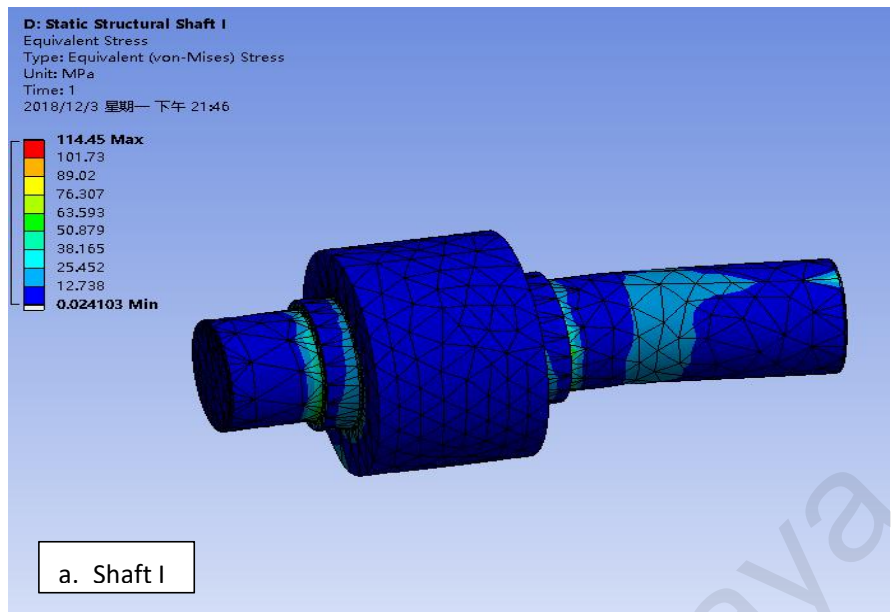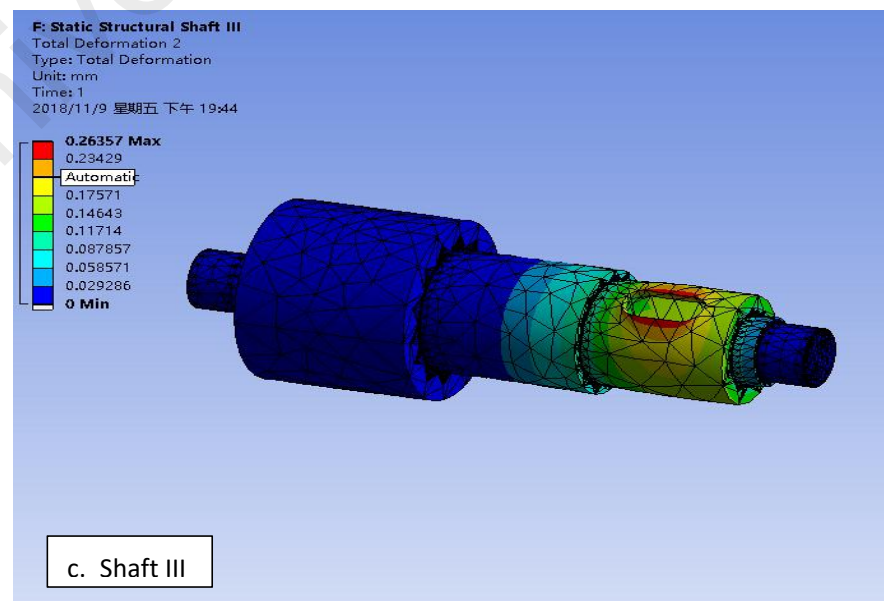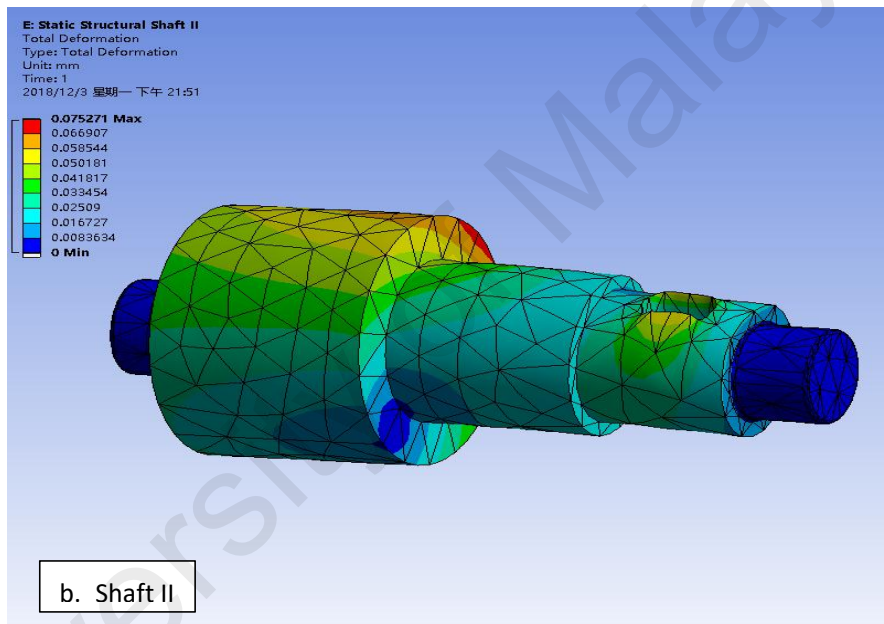The Figure 4.10 to 4.13 of results of shafts are shown below:
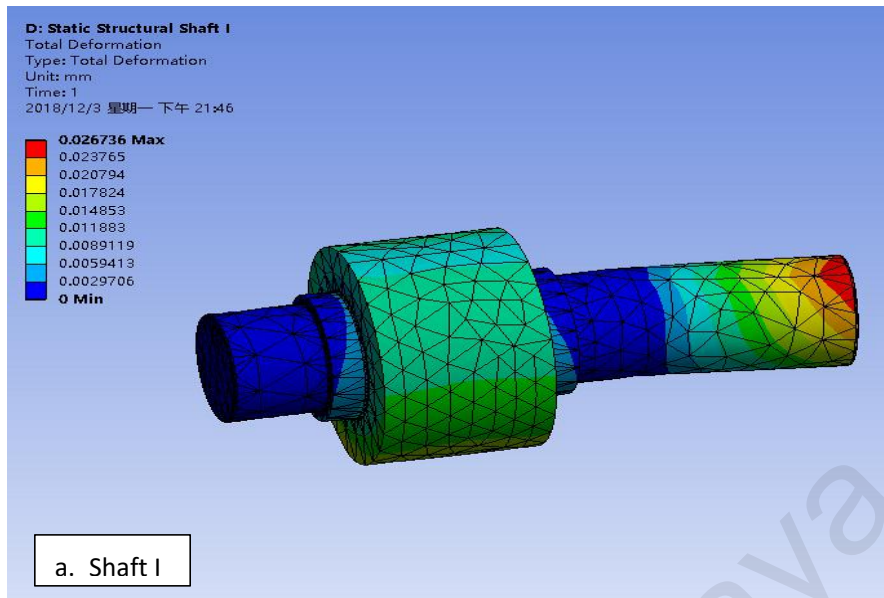
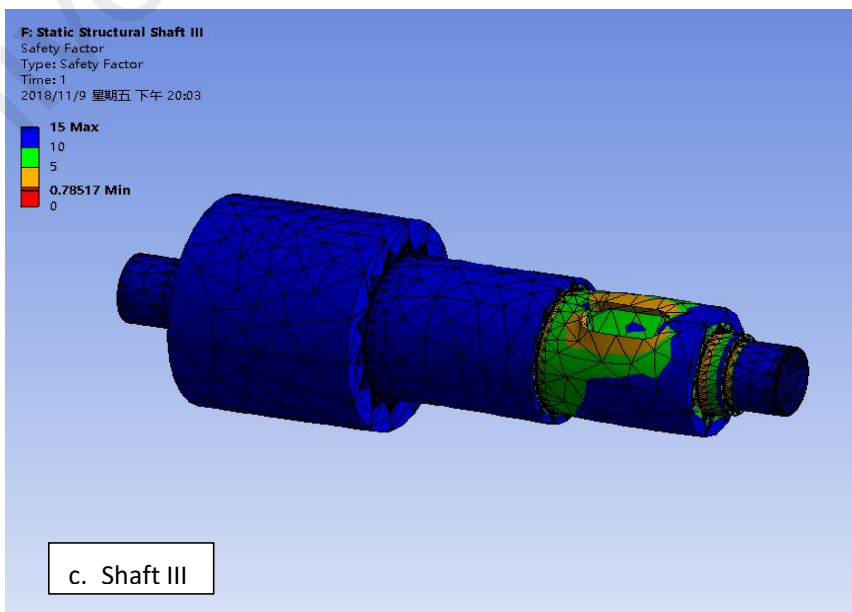Figure 4.10: Maximum equivalent stress of the shafts.

Figure 4.11: Deformation of the shafts.

a. Shaft I

b. Shaft II

c. Shaft III
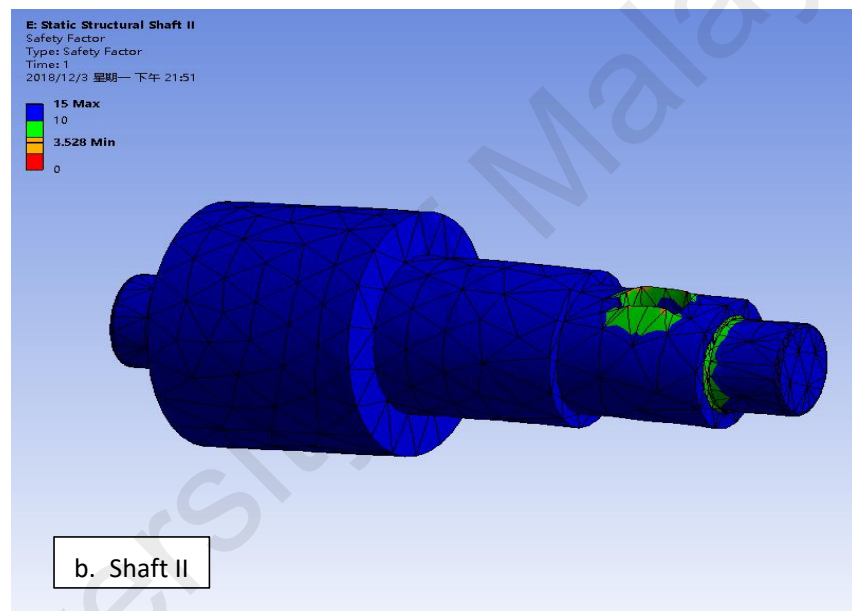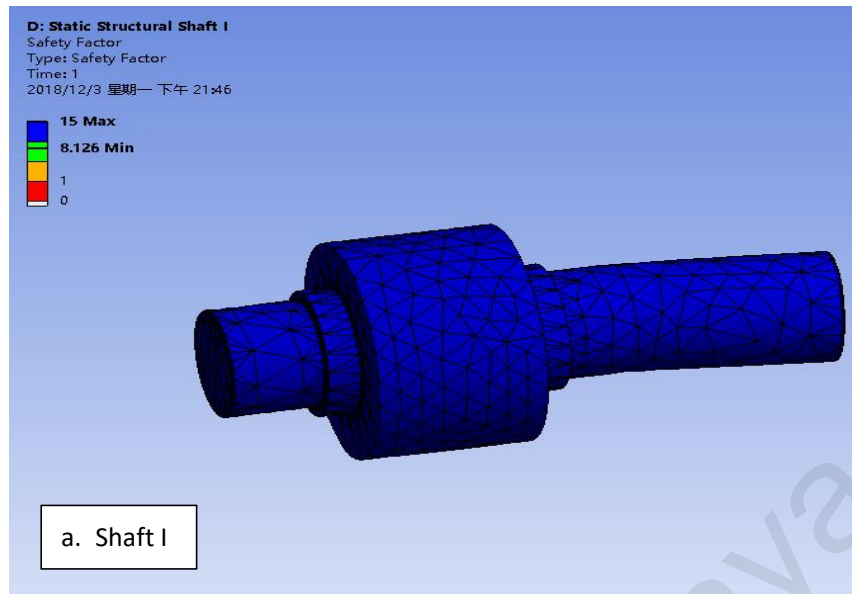
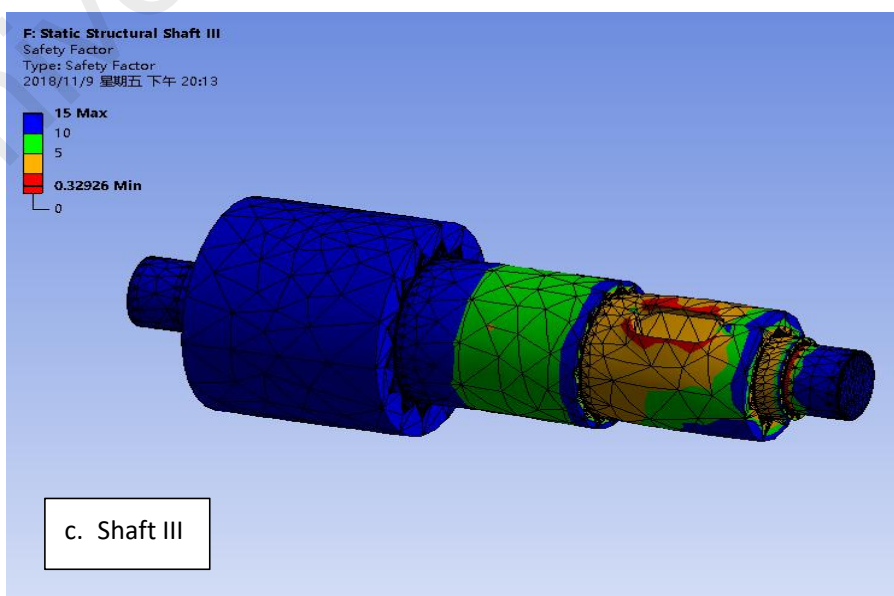Figure 4.12: Safe factor of the shafts from the stress tool.
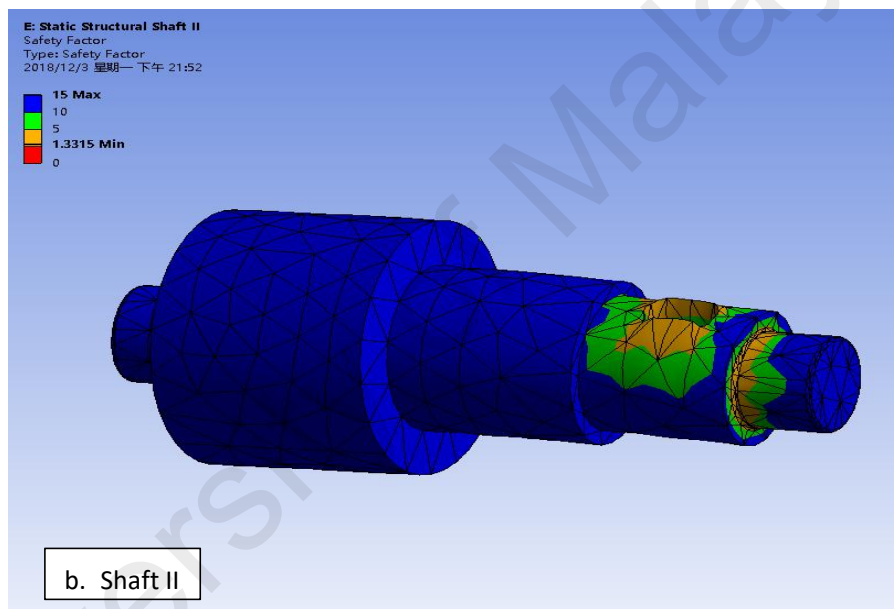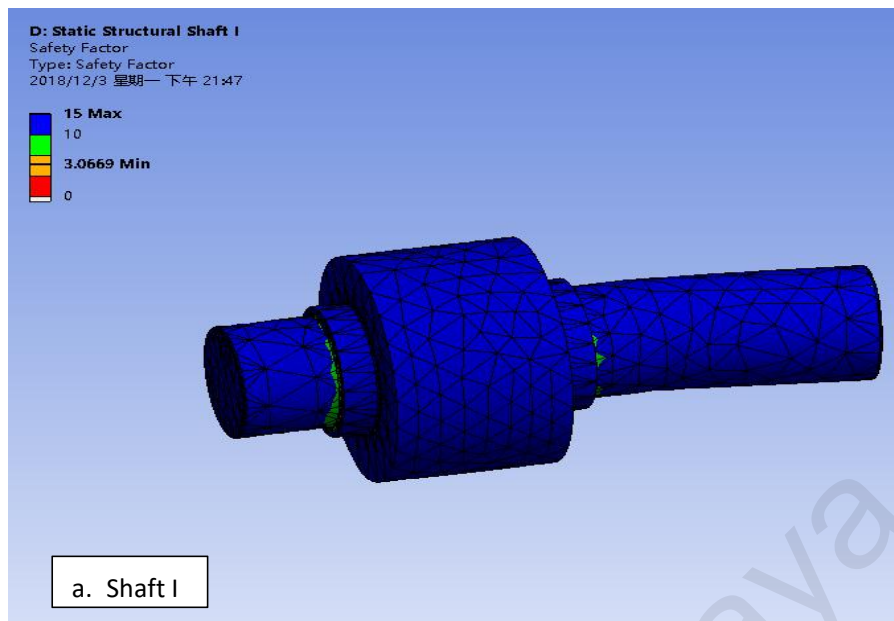
Figure 4.13: Factor of safety of the shafts form fatigue tool.

4.3.2.3 Modal Analysis

The results are calculated for the first 10 modes of each shaft and they are shown on Figure 4.14 below. In Figure 4.14, the minimum frequency of shafts is 44.393 Hz. Reviewing chapter 3, the working frequencies of shafts were shown on Table 3.6, which are not more than 25 Hz, Therefore, the resonance will not happen.

Shaft I;   Shaft II;   Shaft III.
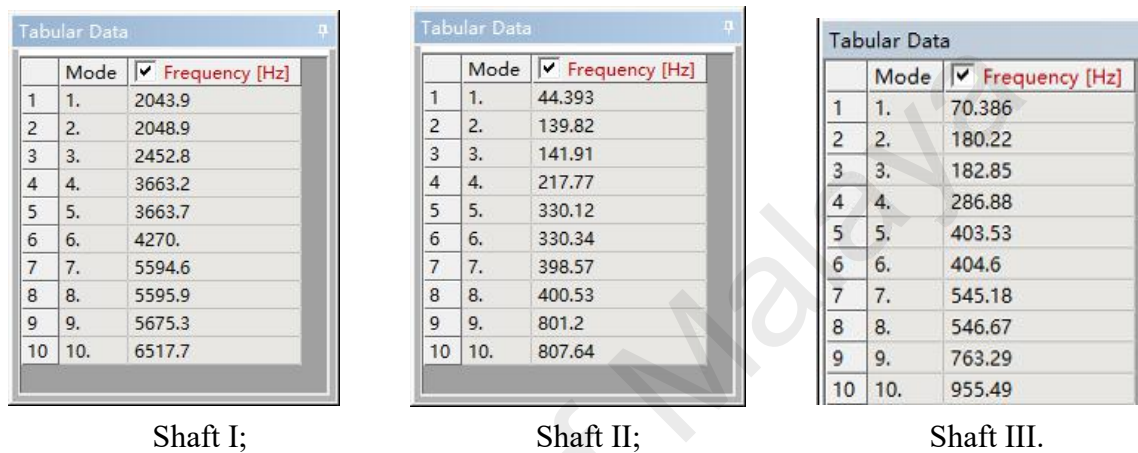
Figure 4.14: Modal analysis of natural frequency of shafts.

4.3.3   Discussion

Comparing the results on Table 4.3 and Table 4.4, the safety factor of shaft I based on Shigley's design method (2.0) is same with that from computational analysis (3.0), which means the shaft I is safe. For shaft II, the yield safety factor 3.7 and fatigue safety factor 1.26 from Shigley's design method are same with yield safety factor 3.528 and fatigue safety factor 1.3315 from computational analysis, which means shaft II is also safe.

However, the safety factor of shaft III from computational analysis is different with the safety factor from Shigley's design method. The safety factor is lower in the results based on computational analysis. I think the reasons of this difference are:

1. The Shigley's design method of shafts is concentrated on analyzing the influence of safety factor from the diameter size, when the load is added uniformly. The influence of local stress concentration on safety is not considered. So the results of safety factor will be greater than that from computational analysis.

2. Computational analysis takes into the influence of stress concentration at keyway, shoulder and fillet, which is a more detailed analysis. Thus, the safety factor is less.

For the failure of shaft III, the problem is mainly concentrated on the bearing position and key way position of this shaft. There is a serious stress concentration in sharp areas. The optimization can be carried out by changing the size of key way and the diameter of bearing position.

4.4 Keys

4.4.1 Results of Shigley's design method

Keys are used on shafts to secure rotating elements, gears. For this speed increaser, the material of keys is 42CrMo, which property is shown on Table 2.2, and the keys are square keys. The factor of safety has been calculated in Chapter 3 and results are shown below on Table 4.5.

Table 4.5: The results of keys based on Shigley's design method.

	The yield safety factor
Key II	3.4
Key III	2.9

As shown in this table, the safety factor of these two keys are above 1.2 (safety factor > 1.2), which verifies that keys can work safely within the design scope.

4.4.2 Results of Computational Analysis

Keys are analyzed by using ANSYS Workbench 18.0 and maximum equivalent stress, deformation of the keys and safe factor of the keys will be analyzed at below on Figure 4.15 to Figure 4.18.

4.4.2.1 Static Analysis

The maximum stress obtained from the solution in ANSYS Workbench on keys is 378.92 MPa (Figure 4.15, b). The maximum deformation is 0.1732 mm (figure 4.16, b). Also, the minimum safety factor of them obtained from the stress tool is 2.4543 (Figure 4.17, b)

4.4.2.2 Fatigue Failure Analysis

The minimum safety factor from fatigue tool is 1.0292 (Figure 4.18, b). Thus, the failure will focus on key III. The problem is mainly concentrated on the fatigue failure.
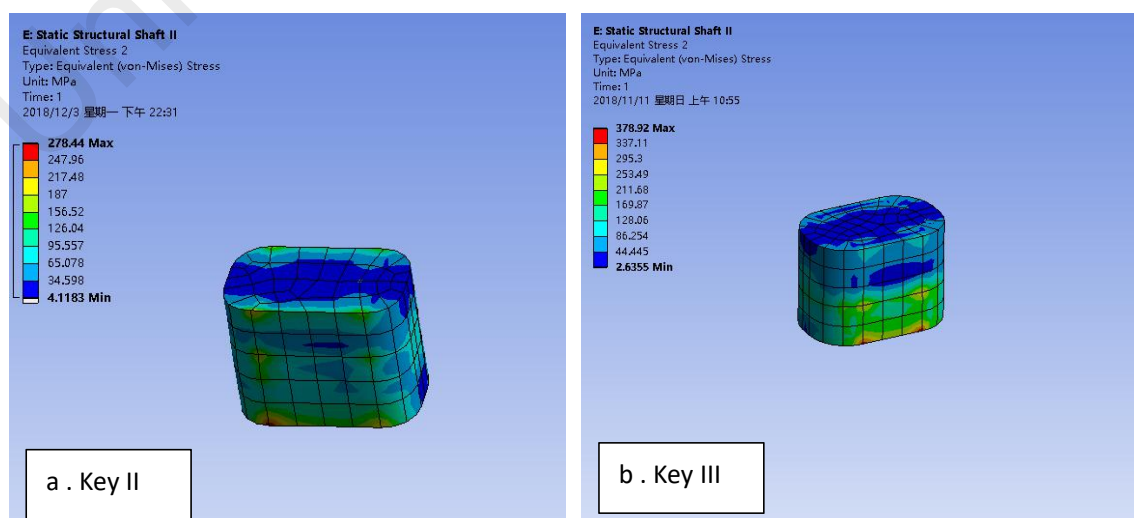

Figure 4.15: Maximum equivalent stress of the keys.
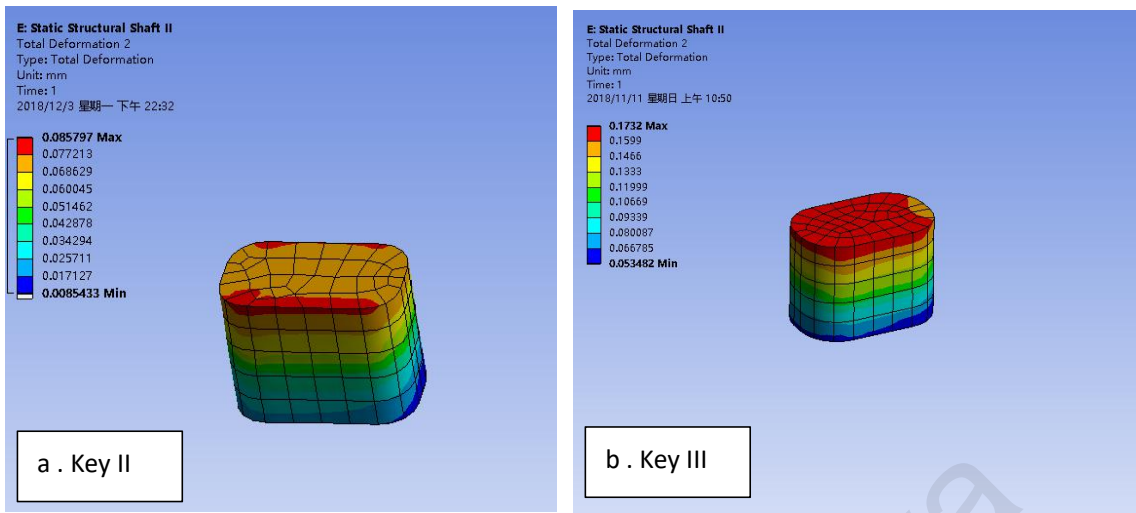
Figure 4.16: Deformation of the keys.
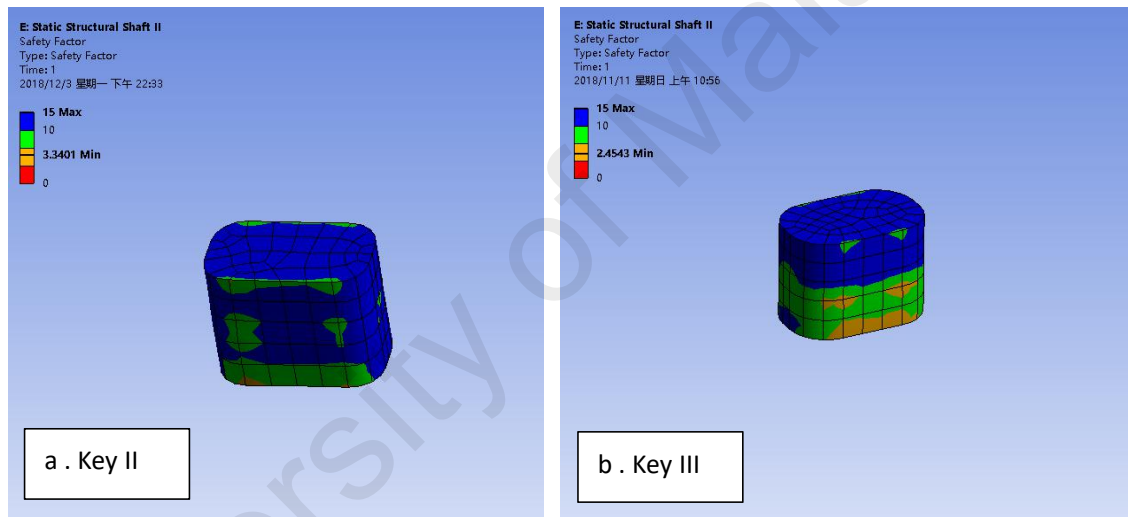
Figure 4.17: Safe factor of the keys from the stress tool.
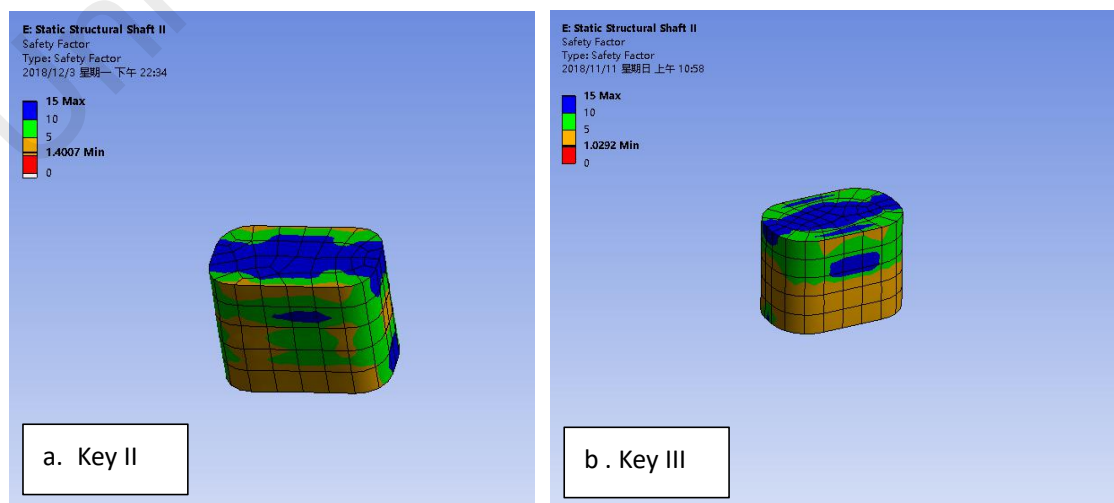
Figure 4.18: Safe factor of the keys from fatigue tool.

The results of computational analysis of keys are shown below on Table 4.6.

Table 4.6: The results of computational analysis of keys

	Maximum Equivalent Stress (MPa)	Max Total Deformation (mm)	Safety factor of Yield Failure	Safety factor of Fatigue Failure
Key II	278.44	0.08579	3.3401	1.4007
Key III	378.92	0.1732	2.4543	1.0292

4.4.3　Discussion

By comparing Table 4.5 and Table 4.6, it can be clearly seen that the yield safety factor both from Shigley's design method and computational analysis are similar, which means there is no yield failure on keys. The fatigue safety factor cannot be calculated by Shigley's design method but computational analysis can. Through the analysis of keys in ANSYS, the fatigue safety factor is 1.4 of key II and 1.0 of key III. Thus, there is a little problem focused on the fillet of Key III. Also, the same problem was found in the keyway position of shaft III. The optimization mainly focuses on the changing dimension of key.

4.5　Bearing

4.5.1　Results of Shigley's design method

Since the bearings on these three shafts are same, in order to verify the safety of bearings at maximum load and maximum speed, the bearing on the left of shaft II is selected. For this bearing, the maximum radial force is 197870 N, and the speed of it is

335 rev/min. The design lift of this bearing is $3.5 \times 10^9 \, cycles$. In addition, the highest speed of these 3 shafts is 1500 rev/min. The basic rated dynamic load C is 906 kN calculated on Chapter 3.

The bearing is selected to SKF cylinder roller bearing that model is NUP 2324 ECML.

Therefore, the basic rated dynamic load C of bearing is 915, which is bigger the 906 calculated before and the reference rotating speed 2800 rev/min is also bigger than the highest speed of all three shafts 1500 rev/min. It means this bearing is safe.

4.5.2   Results of Computational Analysis

To analyze bearing in ANSYS Workbench, the first step is meshing on bearing. The next step is to set fixed support on outer circle of bearing, which can simulate the bearing supported casing. The last step is to add force 197870 N on inter circle of bearing.

4.5.2.1 Static Analysis

The maximum stress obtained from the solution in ANSYS Workbench on bearing is 97.566 MPa (Figure 4.19). Also, the minimum safety factor obtained from the stress tool is 2.5466 (Figure 4.20). Thus, bearing is reasonable and can be used in this speed increaser. Figure 4.19 and Figure 4.20 are shown below.
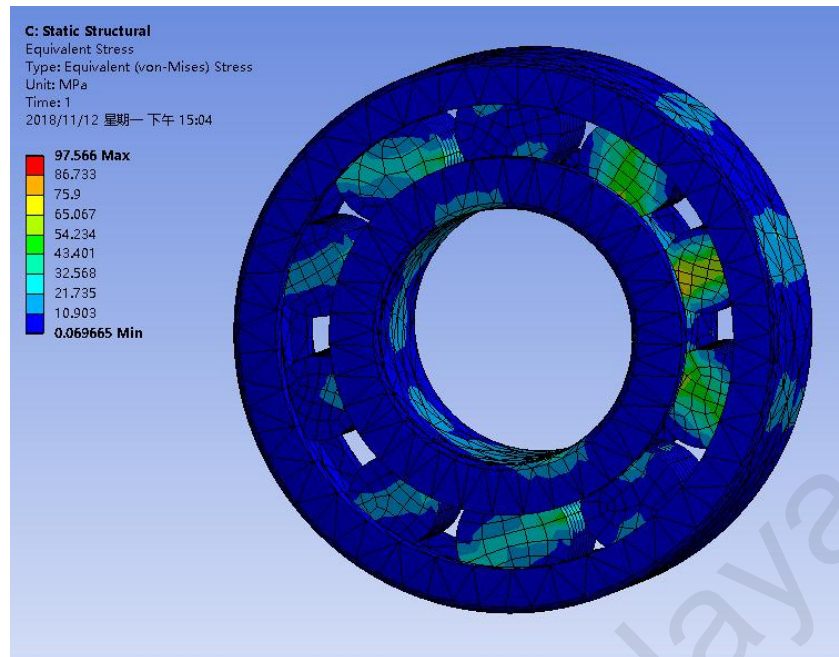
Figure 4.19: Maximum stress of bearing.
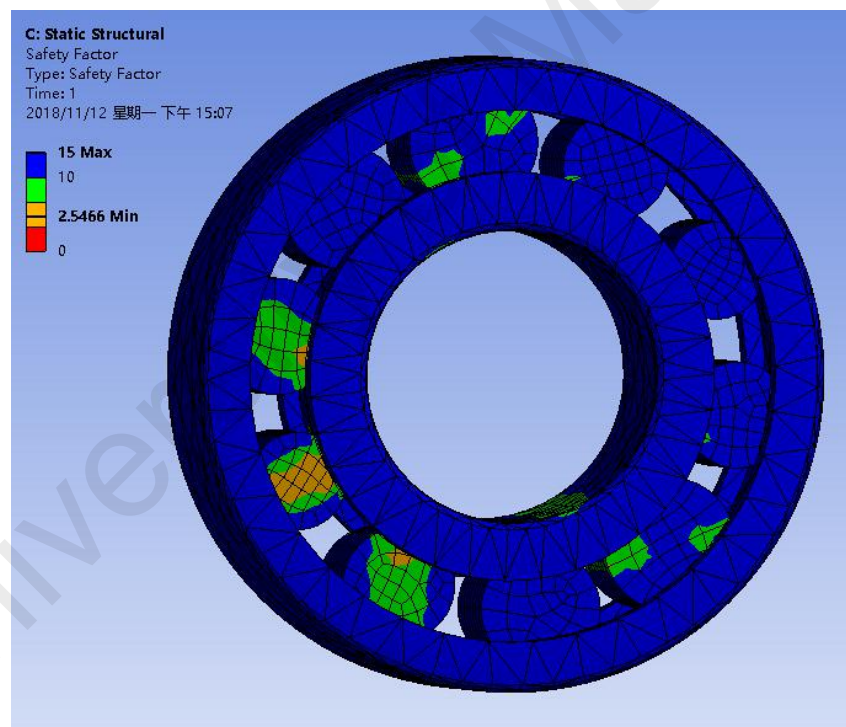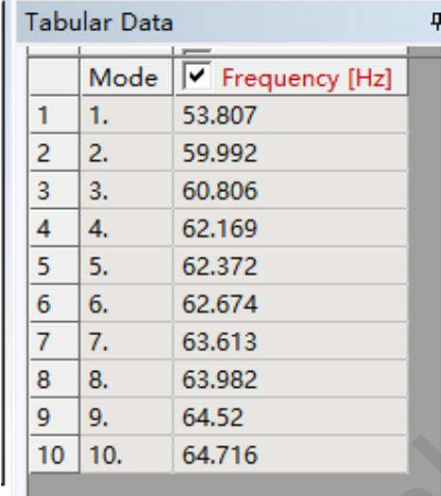
Figure 4.20: Safety factor of bearing from stress tool.

4.5.2.2 Modal Analysis

The results are calculated for the first 10 modes of bearing shown on Figure 4.21 below. In Figure 4.21, the minimum frequency of bearing is 53.807 Hz. Reviewing chapter 3, the working frequencies of shafts were shown on Table 3.6. It shows that the

highest rotational frequency is 25 Hz, which is lower than 53.807 Hz. Therefore, the resonance will not happen.

	Mode	☑ Frequency [Hz]
1	1.	53.807
2	2.	59.992
3	3.	60.806
4	4.	62.169
5	5.	62.372
6	6.	62.674
7	7.	63.613
8	8.	63.982
9	9.	64.52
10	10.	64.716

Figure 4.21: Modal analysis of bearing.

4.6   Casing

4.6.1 Results of Computational Analysis

The material of casing is QT400 gray cast iron and the detail of material was shown on Table 2.2 in chapter 2. In order to simplify the analysis, the first step is to simplify the casing. The simplified method is that removes the gears, shafts and bearings in the casing, and adds a shaft of equal weight into casing. Then, the simple model will be analyzed in ANSYS Workbench 18.0 software.

4.6.1.1 Static Analysis

The static structural analysis method is used to analyze the stress of the casing above self-weight. The most important analysis is the reinforcement and chassis,

because they are the weakest and most vulnerable to failure due to insufficient strength. The result of static structural analysis of casing is shown on Table 4.7.

Table 4.7: Computational analysis results of casing.

	Maximum Equivalent Stress (MPa)	Safety factor of Yield Failure
Casing	11.023	15

The details of results are shown below on Figure 4.22 and Figure 4.23.
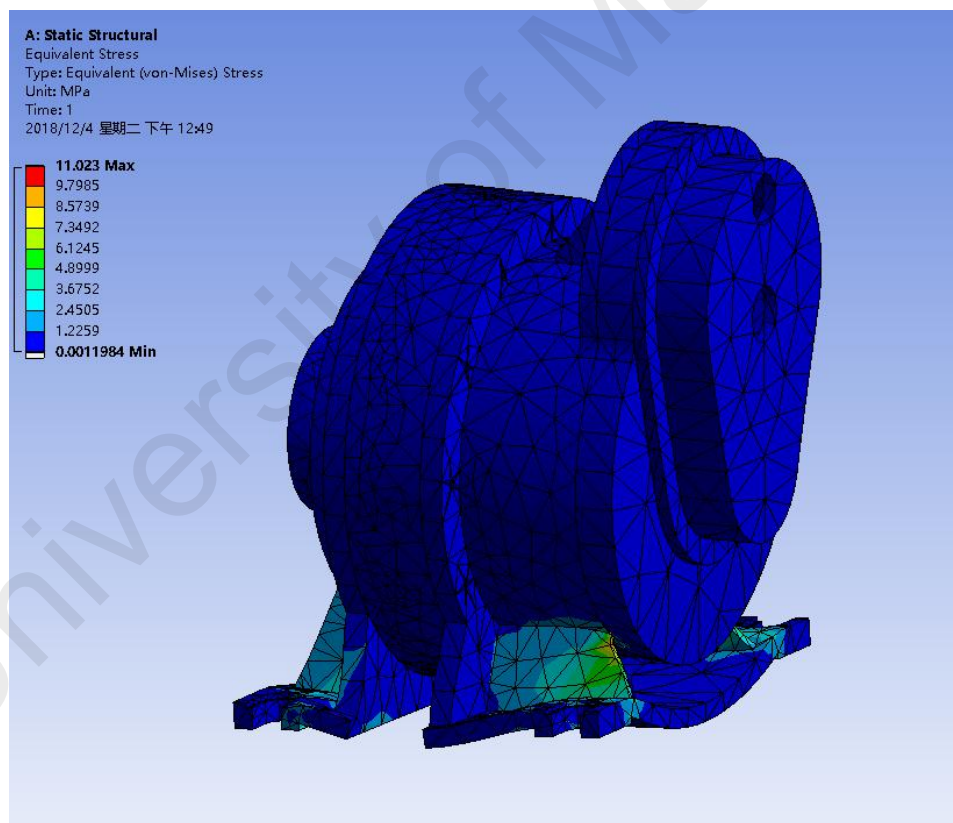
Figure 4.22: Maximum equivalent stress of casing.
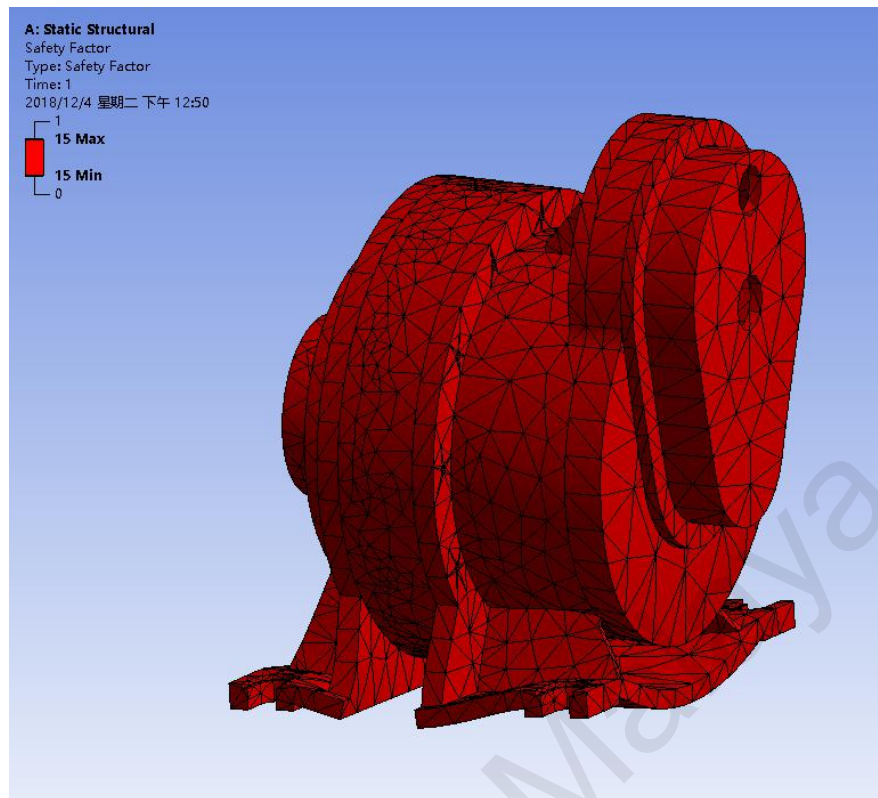
Figure 4.23: Safety factor of casing from stress tool.

4.6.1.2 Modal Analysis

The purpose of modal analysis is to find the natural frequencies of the casing and it can help to obtain the stresses above resonance. The result of modal analysis of casing is shown on Figure 4.24:

Figure 4.24: Modal analysis of casing.

The frequency of each component was shown on Table 3.6. And it's not hard to find that the highest frequency of components is 25 Hz, which is below the smallest frequency of casing 42.041 Hz. Therefore, the resonance will not happen.

4.6.2 Discussion

The maximum stress analyzed by ANSYS is 11.023 MPa, which is very lower than the tensile yield strength of material. And the yield failure safety factor is 15, which means the casing is safe above the force of gravity.

4.7 Parameter Optimization

In this part, design optimization will be performed in ANSYS Workbench 18.0 software. Gears, shafts, keys, bearing and casing have been analyzed by using Shigley's design method and computational analysis methods. All gears, bearing and casing are qualified in both two methods. For shafts and keys, there are problems in shaft III and key III that may cause them to be damaged or to fail before the design life. The common problems of them are large equivalent stress and low safety factor. The parameter optimization will be carried out in ANSYS workbench 18.0 software.

4.7.1 Optimization of Shafts III

The optimization of shaft III is mainly due to changing the diameter and radius of fillet to meet the expected requirements. The sketch of shaft III is shown below on

Figure 4.25. It is clear that D1, D2 and fillet are the 3 parameters need to be optimized.

The original diameters of shaft (D1 and D2) are 120mm; radius of fillet is 3mm.
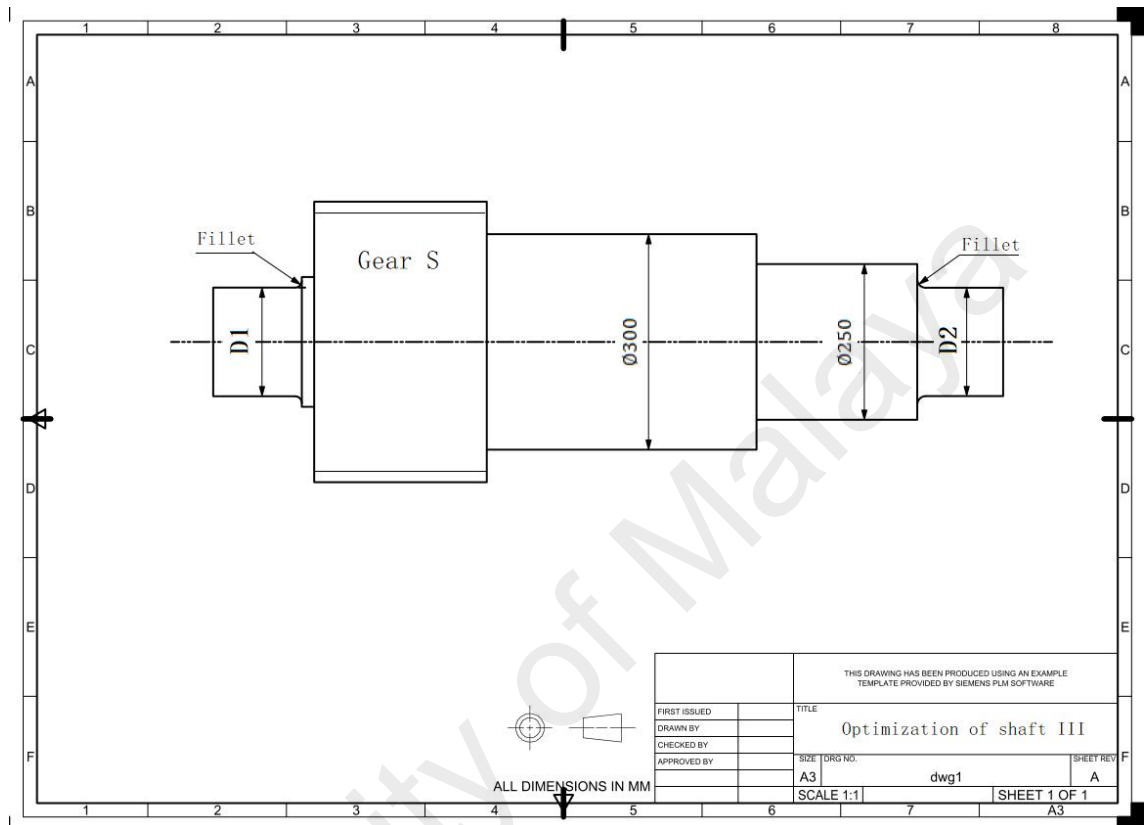
Figure 4.25: The sketch of shaft III.

4.7.1.1 Design of Experiment

The optional ranges of parameters D1, D2 and radius of fillet are input into Design of Experimentation (An optimization function in ANSYS). The boundary set for D1 and D2 is 120mm until 160mm, and the boundary set for radius of fillet is 2.5mm until 6mm. For the output parameter, the maximum equivalent Mises stress, safety factor from stress tool and safety factor from fatigue tool are set. The solution of design of experiment is shown below on Table 4.8.

Table 4.8: Different conditions about input and output parameter.

	Diameter D1 (mm)	Diameter D2 (mm)	Radius of Fillet (mm)	Maximum equivalent stress (MPa)	Safety factor from stress tool	Safety factor from fatigue tool
1	162.5	162.5	4	462.83	2.0	0.84
2	150	162.5	4	414.48	2.2	0.94
3	175	162.5	4	444.43	2.1	0.87
4	162.5	150	4	424.05	2.2	0.91
5	162.5	175	4	319.01	2.9	1.22
6	150	150	3	631.67	1.5	0.62
7	175	150	3	666.48	1.4	0.58
8	150	175	3	384.42	2.4	1.01
9	175	175	3	483.59	1.9	0.81

4.7.1.2 Optimization

In optimization, objectives and constraints are set in advance to achieve desired results. The first concern in optimization is the maximum equivalent Mises stress, which can cause damage to parts. Therefore, equivalent Mises stress must be constrained less than tensile ultimate yield strength of material. Here we set the constraint to: Maximum equivalent stress < 800MPa.

The second constraint is safety factor. In order to ensure the safety of shaft and meet the working life, safety factor is very important and must greater than one. To avoid the safety factor being exactly equal to one, here we set the constraint to: Safety factor from stress tool > 1.2; Safety factor from fatigue tool > 1.2.

Using a simple method based on sampling and classification, the results are obtained through the screening process, and the constraints are associated with all parameters and objectives. Three best candidates are shown below on Table 4.9. Because the maximum

stresses of all candidates are less than 800 MPa, we choose the largest safety factor one. Thus, candidate 2 is the best choice that safety factor from fatigue tool is 1.39. The parameter of candidate 2 will be using for model improve.

Table 4.9: Three best candidates of shaft.

	Candidate 1	Candidate 2	Candidate 3
Maximum equivalent stress(MPa)	340.66	279.64	355.51
Safety factor from stress tool	2.71	3.32	2.67
Safety factor from fatigue tool	1.25	1.39	1.21

4.7.2 Optimization of Key III

The key III is a rectangle key and the optimization of key III is mainly due to changing the length and width to meet the expected requirements. The original length of key is 140mm; with is 57.2mm.

4.7.2.1 Design of Experiment

The optional ranges of parameters length and width are input into Design of Experimentation. The boundary set for length is 135mm until 155mm, and the boundary set for width is 57mm until 70mm. For the output parameter, the maximum equivalent Mises stress, safety factor from stress tool and safety factor from fatigue tool are set. The solution of design of experiment is shown below on Table 4.10.

Table 4.10: Conditions about input and output parameter.

	Length (mm)	Width (mm)	Maximum equivalent stress (MPa)	Safety factor from stress tool	Safety factor from fatigue tool
1	145	63.5	295.66	3.14	1.32
2	135	63.5	337.11	2.76	1.16
3	155	63.5	294.11	3.16	1.33
4	145	57	360.26	2.58	1.10
5	145	70	279.92	3.32	1.40
6	135	57	361.25	2.57	1.08
7	155	57	313.56	2.96	1.24
8	135	70	284.56	3.27	1.37
9	155	70	263.14	3.53	1.48

4.7.2.2 Optimization

For key III, the equivalent Mises stress must be constrained less than tensile ultimate yield strength of material. Here we set the constraint to: Maximum equivalent stress < 800 MPa. To avoid the safety factor being exactly equal to one, here we set the constraint to: Safety factor from stress tool > 1.3; Safety factor from fatigue tool > 1.3.

As in previous steps, three best candidates of key III are shown below on Table 4.11. Because the maximum stress of all candidates is less than 800 MPa, we choose the largest safety factor one. Thus, candidate 3 is the best choice that safety factor from stress tool is 3.53; safety factor from fatigue tool is 1.48. The parameter of candidate 3 will be using for model improve.

Table 4.11: Three best candidates of key.

	Candidate 1	Candidate 2	Candidate 3
Maximum equivalent stress(MPa)	297.22	286.63	263.14
Safety factor from stress tool	3.17	3.27	3.53
Safety factor from fatigue tool	1.33	1.37	1.48

4.7.3 Improved Model and Results

After the parametric optimization of shaft III and key III, the improved model is used to re-analyze to show the performance. Candidate 2 of shaft III and candidate 3 of keyIII are re-analyzed in ANSYS Workbench 18.0. The results and comparison of parameters before and after optimization are shown below on Table 4.12 and Table 4.13.

Table 4.12: Results of re-analysis of shaft III.

Shaft III	Diameter D1 (mm)	Diameter D2 (mm)	Radius of Fillet (mm)	Maximum equivalent stress (MPa)	Safety factor from stress tool	Safety factor from fatigue tool
Before	120	120	3	1184.5	0.78	0.33
After	165	165	5.5	279.64	3.32	1.40

Table 4.13: Results of re-analysis of key III.

Key III	Length (mm)	Width (mm)	Maximum equivalent stress (MPa)	Safety factor from stress tool	Safety factor from fatigue tool
Before	140	57.2	378.92	2.45	1.00
After	155	70	263.14	3.53	1.48

We can see from the tables that dimensions of shaft and key have been optimized, the magnitude of equivalent stress has decreased and all safety factors have reached qualified (safety> 1.2), which means parameter optimization on shaft III and key III is successful.

CHAPTER5: CONCLUSIONS AND RECOMMENDATION

5.1 Conclusions

The purposes of the research is analysis and optimization of speed increaser installed on wind power generation, and the objectives of this project have been achieved. The components of the speed increaser are analyzed by using Shigley's design method and computational analysis methods. The components of speed increaser include gears, shafts, bearing, keys and casing. Shigley's design method is used to calculate the stress and safety factor of each component. Computational analysis using ANSYS Workbench 18.0 software is used for static analysis, fatigue failure analysis and modal analysis of each component. Design optimization is performed on the component which is likely to fail based on the Shigley's design methods and computational analyses.

The models have been built by using UGNX 10.0 software and the dimensions of each component are used in the models successfully. Also, the details of material have been listed and parameters have been filled in this project. Then the models are put into ANSYS for analysis.

The Shigley's design method has calculated the safety factor of gears, shafts, bearing and keys. The analysis has shown that gears, shafts, keys and bearing do not have any failure on Shigley's design method. The safety factors of them are all above 1.2. For gears: the minimum safety factor of these 4 pairs meshing gears is 1.2. For shafts: the minimum safety factor of 3 shafts is 1.2. For keys: the minimum safety factor of 2 keys is 2.9. There is also no failure on bearing based on Shigley's design method.

The computational analysis has analyzed the maximum equivalent stress, safety factor from stress tool and safety factor from fatigue tool of gears, shafts, keys, bearing and casing. All gears do not show any failure based on the static analysis and dynamic analysis. The maximum equivalent stress, minimum safety factor from stress tool and safety factor from fatigue tool of these 4 pairs meshing gears are 132.29 MPa, 7.03 and 2.65 respectively. Shaft III has is likely to fail. The failure is mainly due to the stress concentration in the sharp area and strength failure. The maximum stress of shaft III reaches 1184.5 MPa, and the safety factor from stress tool and fatigue tool are 0.78 and 0.33 respectively, which is below 1.2. For keys, there is fatigue failure on key III. The safety factor from fatigue tool is 1.03. Bearing and casing do not show any failure with safety factor of 2.55 and 15 respectively.

In design optimization, the main objective is to avoid high equivalent stress and low safety factor. In chapter 4, shaft III and key III are optimized by using ANSYS software. The equivalent stress of shaft III has been reduced from 1184.5 MPa to 297.64 MPa, and the safety factors from stress tool and fatigue tool show increment from 0.78 to 3.32 and 0.33 to 1.4 respectively. The fatigue safety factor of key III has also increased to 1.48. Thus, the design optimization has solved the problem.

In conclusion, this study has analyzed the speed increaser successfully by using Shigley's design method and computational methods. And design optimization helps to improve reliability.

5.2   Recommendation

The following are some recommended steps that can be taken into consideration in future research work. Further extension on the research which can be conducted includes:

1. Although in the process of modeling the speed-increasing box of wind turbines, a lot of conditions in its actual operation are also taken into account. However, the working environment of the fan is quite complex, and the model of the fan speed-increasing box established has some errors with the actual working state.

2. In this project the gears, shafts and keys in the gearbox are analyzed, but other types of faults are not studied in depth.

REFERENCE

Bao, E. (2004). Development of wind power technology. *Journal of renewable energy*. *32*(2), 1-12. Retrieved from http://www.docin.com/p-1139737242.html

Crabtree, C. J., Feng, Y., & Tavner, P. J. (2010). Detecting Incipient Wind Turbine. Gearbox Failure: A Signal Analysis Method for On-line Condition Monitoring. *Journal of Organic Chemistry*, *75*(18), 6122-6140. Retrieved from https://doi.org/10.1051/matecconf/201819804008

Dong, H. M., Ding, S. & Wang, H. Y. (2014). Research on lightweight design database of saddles. *Modular machine tools and automatic processing technology*, (3), 33-36. DOI: 10.13462/j.cnki.mmtamt.2014.03.009

Dong, J. Z. (2007). Research on Key Design Technologies of Large Wind Power Gearbox (Doctoral dissertation). DOI: 10.7666/d.Y1172149

Fui, T. H., & Rahman, R. A. (2007). Statics and dynamics structural analysis of a 4.5 ton truck chassis. *Jurnal Mekanikal, 24*(2). Retrieved from https://jurnalmekanikal.utm.my/index.php/jurnalmekanikal/article/view/162

Fuglsang, P., & Madsen, H. A. (2000). Optimization method for wind turbine rotors. *Journal of Wind Engineering and Industrial Aerodynamics, 80*, 191-206. https://doi.org/10.1016/S0167-6105 (98)00191-3

Gokhale, N. S. (2008). Practical finite element analysis: Finite to infinite.

Guo, X. W. (2012). Research on lightweight structure of megawatt wind power gearbox (Doctoral dissertation). Retrieved from http://xueshu.baidu.com/usercenter/project/show?projectid=e72fb1daef14593654 1f1114853c78dd&site=xueshu_se

Jan, H., Frederik, V. & Filip, D. C. (2011). Insights in wind turbine drive train dynamics gathered by validating advanced models on a newly developed 13.2 MW dynamically controlled test-rig. *Mechatronics, 21*(4), 737-752. https://doi.org/10.1016/j.mechatronics.2010.11.005

Liu, G. (2004). Three-dimensional contact stress analysis of internal spur gears. *Journal of Computational Mechanics, 11* (1), 63-67. Retrieved from http://xueshu.baidu.com/usercenter/project/show?projectid=a8bc8c3d312afc9f6fd aedd65ba4dee7&site=xueshu_se

Liu Zhe (2010). Design and Simulation of wind turbine accelerator (Doctoral dissertation, Wuhan University of Technology). DOI: 10.7666/d.y1685225

Litvin, F. L., Fuentes, A., & Vecchiato, D. (in press). Design of Gear Drives with High Gear Ratio. *NASA Technical Report.*

Luo, H. T., Wang, C. J., Meng, J. H., & Zong, X. (2006). Digital design method of mechanism system. *Mechanical engineering and automation, 39*(5), 41-43. DOI: 10.3969/j.issn.1672-6413.2006.05.016

Lee, Y., Zhu, C. Z., & Tao, Y. C. (2017). Research status and development trend of wind turbine reliability. *China Mechanical Engineering*, *28*(9), 1125-1133. DOI: 10.3969/j.issn.1004-132X.2017.09.021

Lin, J., & Parker, R. G. (2002). Planetary gear parametric instability caused by mesh stiffness variation. *Journal of Sound and Vibration*, *249*(1), 129-145. Retrieved from https://doi.org/10.1006/jsvi.2001.3848

Mao, F. H., Han, M. K. & Dong, H. M. (2015). A lightweight design for the front body structure of megawatt wind power gearbox. *Mechanical transmission*, (11), 50-53. Retrieved from http://xueshu.baidu.com/usercenter/project/show?projectid=5bce6d67cfc2f10ad68abb6a4c349b52&site=xueshu_se

Ma, C., Ma, Y. L. & Zhao, H. A. (2011). Static and dynamic optimization and lightweight design of column structure of Vht800 vertical turning and milling machining center. *Modular machine tools and automatic processing technology, 39*(3), 11-15. DOI: 10.3969/j.issn.1001-2265.2011.03.004

Mabie, H. H., & Reinholtz, C. F. (1987). *Mechanisms and Dynamics of Machinery. 4th edition.* New York: Published by Wiley.

Parey, A., & Tandon, N. (2003). Spur Gear Dynamic Models Including Defects: A Review. *The Shock and Vibration Digest*, *35*, 465-478. DOI: 10.1177/05831024030356002.

Parker, R. C. (2010). Mesh Phasing for Epicyclic Gear Vibration. Proceedings of the International Conference on Mechanical Transmission (Doctoral dissertation). Retrieved from http://www.jasp.com.cn/ch/reader/view_abstract.aspx?file_no=20030228

Parker, R. G., & Kiracofe, D. (2007). Structured vibration modes of general compound planetary gear systems. *Journal of Vibration and Acoustics, 129*(1): 1-16. doi:10.1115/1.2345680

Qin, D. T, Xing, Z. K. & Wang, J. H. (2008). Parameter optimization design of wind power gear transmission system based on dynamics and reliability. *Journal of Mechanical Engineering, 32* (7), 55-56. DOI: 10.3321/j.issn:0577-6686.2008.07.004

Ragheb, Adam., & Ragheb, M. (2010). Wind turbine gearbox technologies, *1st International Nuclear & Renewable Energy Conference (INREC)*, pp. 1-8. DOI: 10.1109/INREC.2010.5462549

Rossow, W. P., & Taylor, J. E. (2007). A finite element method for the optimal design of variable thickness sheets. *J.E. TAYLOR AIAA Journal*, *11*(11), 1566-1569. Retrieved from https://arc.aiaa.org/doi/abs/10.2514/3.50631?journalCode=aiaaj

Richard, G. B., & Nisbett, J. K. (2010). *Shigley's Mechanical Engineering Design 9th Edition*. Malaysia: Mc Graw.

Sui, Y. K. (1996). Modeling, transformation and Optimization: new progress in structural synthesis methods. *Dalian University of Technology press*.

She, B. Q. (2008). Research on Wind Power Increasing Device. *Dissertation of Xi'an University of technology.* DOI: 10.7666/d.y1380893

Tong, L. J. (2010). Gear transmission dynamics analysis based on ansys/ls-dyna. *Tractors and farm transporters, 37* (2), 33-34. DOI: 10.3969/j.issn.1006-0006.2010.02.013

Vaishya, M., & Singh, R. (2001). Sliding friction-induced non-linearity and parametric effects in gear dynamics. *Journal of Sound and Vibration*, *248*(4), 671-694. https://doi.org/10.1006/jsvi.2001.3818

Wang, J. J., & Wu, X. L. (2008). Development and technical analysis of wind turbine gearbox. *Mechanical Transmission, 32*(6), 5-8. DOI: 10.3969/j.issn.1004-2539.2008.06.002

Wu, J. L. (2005). Finite element modal analysis of cylindrical gears. *Coal mining machinery, 32*(10), 60-61. DOI: 10.3969/j.issn.1003-0794.2005.10.026

Yang, W. & Han, G. S. (2007). Study on Nonlinear Three-Dimensional Contact Dynamic Characteristics of Bearing-Gear Shafting of Microcap Transmission. *Vibration and IMPact, 26* (11), 9-12. DOI: 10.3969/j.issn.1000-3835.2007.11.003

Zhao, X., Liang, Y. W. & Lee, S. S. (2009). Dynamic contact simulation analysis of helical gears based on ls-dyna. *Mechanical engineering and automation*, *39* (3), 9-11. DOI: 10.3969/j.issn.1672-6413.2009.03.004

Zhan, Z. (2003). Wind turbine transmission. *Transmission technology, 17* (2), 35-36. DOI: 10.3969/j.issn.1006-8244.2003.02.004